Synthesis of Triphenylethylene Bisphenols as Aromatase Inhibitors that Also Modulate Estrogen Receptors

Wei Lv,[†] Jinzhong Liu,[‡] Todd C. Skaar,[‡] Elizaveta O'Neill,[†] Ge Yu,[†]

David A. Flockhart,[‡] and Mark Cushman[*,†]

[†]Department of Medicinal Chemistry and Molecular Pharmacology, College of Pharmacy, and The Purdue University Center for Cancer Research, Purdue University, West Lafayette, Indiana 47907, United States

[‡]Division of Clinical Pharmacology, Department of Medicine, Indiana University School of Medicine, Indianapolis, Indiana 46202, United States

---

This is the author's manuscript of the article published in final edited form as:
Lv, W., Liu, J., Skaar, T. C., O'Neill, E., Yu, G., Flockhart, D. A., & Cushman, M. (2016). Synthesis of Triphenylethylene Bisphenols as Aromatase Inhibitors That Also Modulate Estrogen Receptors. Journal of Medicinal Chemistry, 59(1), 157–170. http://doi.org/10.1021/acs.jmedchem.5b01677

Abstract

A series of triphenylethylene bisphenol analogues of the selective estrogen receptor modulator (SERM) tamoxifen were synthesized and evaluated for their abilities to inhibit aromatase, bind to estrogen receptor-α (ER-α) and estrogen receptor-β (ER-β), and antagonize the activity of β-estradiol in MCF-7 human breast cancer cells. The long-range goal has been to create dual aromatase inhibitor (AI)/selective estrogen receptor modulators (SERMs). The hypothesis is that in normal tissue the estrogenic SERM activity of a dual AI/SERM could attenuate the undesired effects stemming from global estrogen depletion caused by the AI activity of a dual AI/SERM, while in breast cancer tissue the antiestrogenic SERM activity of a dual AI/SERM could act synergistically with AI activity to enhance the antiproliferative effect. The potent aromatase inhibitory activities and high ER-α and ER-β binding affinities of several of the resulting analogues, together with the facts that they antagonize β-estradiol in a functional assay in MCF-7 human breast cancer cells and they have no E/Z isomers, support their further development in order to obtain dual AI/SERM agents for breast cancer treatment.

INTRODUCTION

Aromatase (also known as CYP19) is a member of the general class of cytochrome P450 enzymes. It catalyzes the conversion of androgens to estrogens, which is a crucial step in the biosynthesis of estrogens in the human body.[1] Aromatase inhibitors (AIs) have been widely used for treatment of hormone receptor-positive breast cancer in postmenopausal women. Currently, three AIs [letrozole (**1**), anastrozole (**2**) and exemestane (**3**), Figure 1] have been approved by the FDA. Comparative clinical trials involving postmenopausal women with breast cancer have demonstrated that AIs are superior to the selective estrogen receptor modulator (SERM) tamoxifen (**4**) (Figure 1), which, as with other SERMs, blocks estrogen receptors in breast cancer tissue while stimulating them in a variety of normal tissues.[2-6] In the five-year ATAC (Arimidex, Tamoxifen, Alone, or in Combination) trial, the use of anastrozole alone resulted in a 13% improvement of disease-free survival, 21% reduction in the time-to-recurrence, 42% reduction in occurrence of contralateral breast cancer and 14% reduction in risk of distant metastasis when compared to tamoxifen alone.[4] The use of AIs is also reported to cause fewer vaginal bleeding events, thromboembolic events, and endometrial cancer occurrences than tamoxifen.[4-6] However, the use of AIs is associated with serious side effects. Since AIs nonselectively deplete estrogen in the whole body, they lead to severe musculoskeletal pain, reduction of bone density, and an increased frequency of bone fractures and cardiovascular events.[7-11] According to the five-year ATAC trial, anastrozole treatment led to a higher incidence of bone fractures (11% vs 7.7%) and arthralgia (35.6% vs 29.4%) than tamoxifen.[4] The increased musculoskeletal pain caused by AIs negatively impacts patient compliance. Reported AI discontinuation rates attributed to severe musculoskeletal symptoms range from 13-52%.[12-14] Non-adherence rates are also high.[15, 16] For

example, observations from three data sets indicate that only 62-79% of women adhere (take anastrazole more than 80% of the days during the treatment period) after three years.[16]

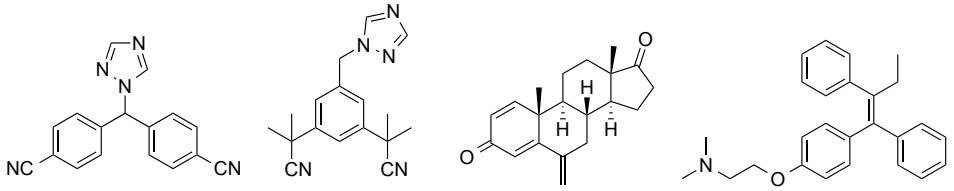

Figure 1. The structures of the aromatase inhibitors letrozole, anastrozole, exemestane, and the selective estrogen receptor modulator tamoxifen.

One possible approach to improve the efficacy and decrease the side effects associated with AIs is to build SERM activity into them. The estrogenic activity of a dual AI/SERM due to binding to and stimulation of estrogen receptors (ERs) in non-cancerous musculoskeletal tissue could counteract some of the negative effects of the dual AI/SERM that result from global estrogen loss due to aromatase inhibition. On the other hand, the antagonistic blockade of ERs in breast cancer cells by a dual AI/SERM might act synergistically with the decrease in estrogen concentration due to aromatase inhibition, assuming that the inhibition of estrogen production is not totally complete. In other words, as with the SERMs, the ER agonist effect of a dual AI/SERM would be beneficial in normal, non-cancerous musculoskeletal tissue relative to an AI alone by decreasing the side effects that result from estrogen depletion, while the ER antagonist effects of a dual AI/SERM would be beneficial in breast cancer cells by blocking the effect of residual estrogen resulting from incomplete aromatase inhibition. In fact, according to Brodie et al., a combination of the aromatase inhibitor letrozole and the estrogen receptor antagonist/down-regulator fulvestrant was more effective than either letrozole or fulvestrant alone in suppressing

breast tumor growth and in delaying the development of tumor resistance.[17-19] In that case, the delay in development of resistance was thought to result from down-regulation of the ER by fulvestrant and an associated down-regulation of signaling proteins that play a role in the maintenance of hormonal resistance.[19] Meanwhile, it is also possible that the estrogenic component of the SERM activity of a dual AI/SERM agents could stimulate estrogen receptors in non-cancerous musculoskeletal tissues and ameliorate the side effects caused by estrogen depletion of conventional AIs (e.g. osteoporosis, musculoskeletal pain, and bone fractures). In fact, according to the ATAC trail, a combination of anastrozole with tamoxifen resulted in fewer fractures than when anastrozole was used alone.[20] As expected, the combination resulted in more fractures than tamoxifen alone, indicating that the fractures were the result of the AI and not the SERM.[20] For these reasons, dual AI/SERM agents could possibly have superior efficacy and decreased side effects compared to conventional AIs alone. However, the combination of anastrozole with tamoxifen resulted in a greater incidence of endometrial cancer (0.3%) than anastrozole alone (0.1%), and in this regard it may be better to combine raloxifene-type SERM activity than tamoxifen-type SERM activity with an AI (different SERMs produce unique spectra of agonist activities in different normal tissues because they have different affinities for ER-α and ER-β, which are expressed to different extents in various tissues, and the consequences of binding to ER-α and ER-β are different).[21] Although the ATAC trial showed no therapeutic advantage of a specific tamoxifen plus anastrozole combination with regard to anticancer activity,[20] this result should not be generalized to all SERM plus AI combinations or to a hypothetical dual AI/SERM agent. Of note, the serum concentration of anastrozole, a relatively weak aromatase inhibitor, was 27% lower in the combination arm of the ATAC trial, although it was claimed that this was of no pharmacological significance.[22]

Norendoxifen is a metabolite of tamoxifen, and it is also a potent aromatase inhibitor.[23] The synthesis of (*E,Z*)-norendoxifen (**5**) was reported in 2013.[24] Biological testing results confirmed the aromatase inhibitory activity of (*E,Z*)-norendoxifen and further established high affinity for both ER-α and ER-β (Figure 2), establishing (*E,Z*)-norendoxifen the first substance with potential dual AI and ER binding activity.[24, 25] The *E*- and *Z*-norendoxifen isomers (***E*-5** and ***Z*-5**) were also prepared via stereoselective synthetic routes, and their biological activities revealed that *E*-norendoxifen is the more potent aromatase inhibitor, while *Z*-norendoxifen displayed greater affinity for both ER-α and ER-β.[24] To optimize efficacy and CYP selectivity, a series of norendoxifen analogues were subsequently designed and prepared using a structure-based drug design approach. This led to the discovery of 4'-hydroxynorendoxifen (**6**), which has elevated potency against aromatase and higher affinity for ER-α and ER-β. It is also a more potent antagonist of estradiol-stimulated progesterone receptor mRNA expression in MCF-7 cells compared to norendoxifen.[26]

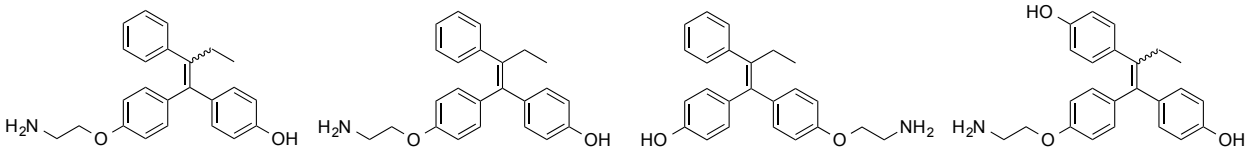

5 (E/Z=1:1)
(*E,Z*)-Norendoxifen
Aromatase IC_{50} = 102 nM
Aromatase K_i = 77 nM
ER-α EC_{50} = 27 nM
ER-β EC_{50} = 35 nM

***Z*-5** (E/Z = 1:10)
***Z*-Norendoxifen**
Aromatase IC_{50} = 1030 nM
Aromatase K_i = 442 nM
ER-α EC_{50} = 17 nM
ER-β EC_{50} = 28 nM

***E*-5** (E/Z > 100)
***E*-Norendoxifen**
Aromatase IC_{50} = 77 nM
Aromatase K_i = 48 nM
ER-α EC_{50} = 59 nM
ER-β EC_{50} = 79 nM

6 (E/Z=1:1)
4'-Hydroxynorendoxifen
Aromatase IC_{50} = 45 nM
Aromatase K_i = 20 nM
ER-α EC_{50} = 15 nM
ER-β EC_{50} = 9.5 nM

Figure 2. The structures and biological activities of (*E,Z*)-norendoxifen, *Z*-norendoxifen, *E*-norendoxifen and 4'-hydroxynorendoxifen.

Like 4-hydroxytamoxifen, most norendoxifen analogues undergo facile E/Z isomerization in solution.[24] Although the detailed mechanism is still controversial, the E/Z isomerization is considered to be facilitated by the presence of a phenolic hydroxyl group in one of the para positions.[27] The rate of isomerization speeds up as the number of para phenolic hydroxyl group increases, and the rate is also dependent on the solvent and temperature.[28] The E/Z isomerization makes the preparation of pure E and Z isomers of norendoxifen analogues difficult. Moreover, since isomerization happens both in stock solutions and during biological testing, it also influences the accuracy of the biological testing results for pure E and Z isomers. To develop more promising norendoxifen analogues for treatment of breast cancer, it is important to prepare analogues as pure E and Z isomers. A mixture of E and Z isomers would complicate the pharmacological profiles and limit the use of the drugs because the E and Z isomers would be expected to have different biological activities against aromatase, ERs and other CYPs. This argument is in fact supported by results derived from testing tamoxifen, which document different relative binding affinities of the two isomers for the ER, as well as different agonist vs. antagonist properties as monitored by uterine weight.[29] Furthermore, the isomerization of (*Z*)-4-hydroxytamoxifen to its less active isomer is thought to contribute to tamoxifen resistance.[30]

To overcome the problem presented by E/Z isomerization, a series of triphenylethylene bisphenol analogues were designed by eliminating the aminoethoxy side chain of norendoxifen, thus resulting in two identical substituents on one end of the double bond and eliminating the possibility of E/Z isomers. This allowed a straightforward evaluation of the aromatase inhibitory activities, ER-α and ER-B binding affinities, and abilities of the compounds to antagonize β-estradiol-stimulated transcriptional activity in MCF-7 human breast cancer cells. The results of

these studies will facilitate the development of a new generation of dual AI/SERM agents for breast cancer treatment.

RESULTS AND DISCUSSION

Design of Triphenylethylene Bisphenol Analogues. Compound **7** is a weak aromatase inhibitor, and it also shows moderate binding affinities to ER-α and ER-β (Table 1).[24] This substance is also a good ER antagonist without significant agonistic side effects in MCF-7-2a cells.[31] Based on the structure of compound **7**, the following structural modifications were explored to improve the potency (Figure 3). (1) Incorporation of hydrogen bond donors (hydroxyl or amino groups) on the meta or para positions of the "A" ring. (2) Introduction of iron-coordinating groups (nitrile, imidazole or triazole groups) in the location of the ethyl group. Hydrogen bond donors on the "A" ring can be expected to form hydrogen bonds with aromatase and the ERs, while iron-coordinating groups could improve aromatase inhibitory activity by coordinating to the iron of aromatase.

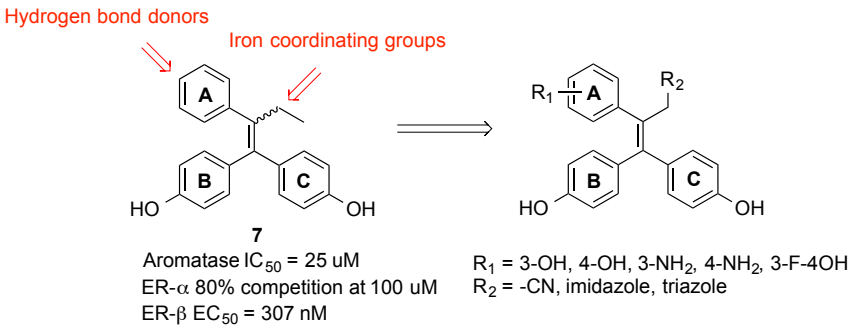

Figure 3. The design strategy for triphenylethylene bisphenol analogues.

Synthesis. A short and efficient synthetic route was established to prepare analogues with an iron-coordinating group in the location of the ethyl side chain (Scheme 1). The bisphenol **9** was

first prepared by McMurry cross-coupling of acetophenone (**8**) with 4,4'-dihydroxybenzophenone as described.[25] The bisphenol **9** was treated with an excess of MOMCl to afford the di-protected product **10** in good yield. The protected intermediate **10** underwent a series of reactions, including bromination with NBS, alkylation of potassium cyanide, and deprotection of the MOM groups with HCl to afford the nitrile **11** in very good yield. The imidazole product **12** and triazole compound **13** were also obtained in good yield by treating **10** with similar sequential reactions, including bromination with NBS, alkylation of imidazole or 1,2,4-triazole, and cleavage of the phenols.

Scheme 1. Synthesis of Analogues 11-13[a]

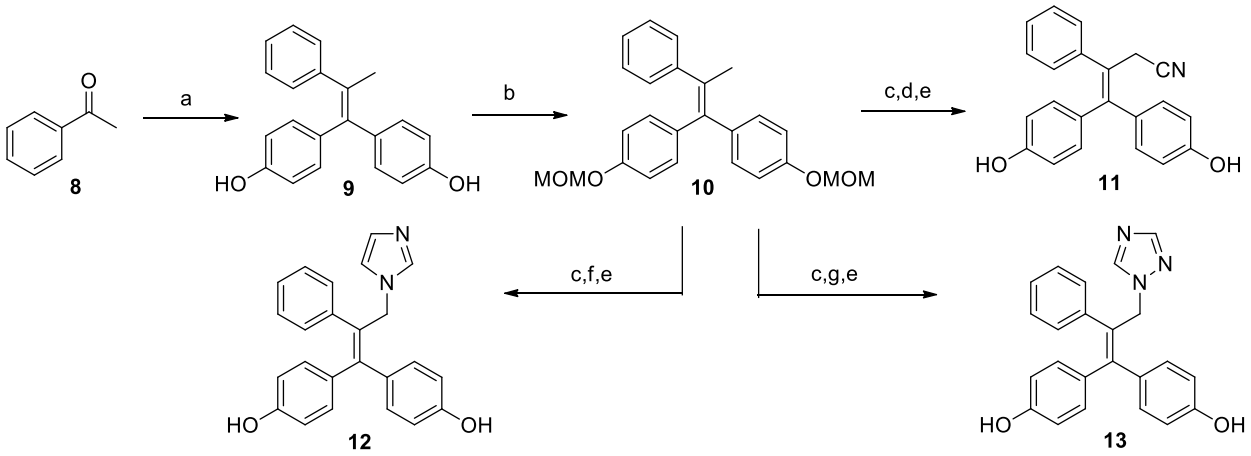

8 **9** **10** **11** **12** **13**

[a]Reagents and conditions: (a) 4,4'-dihydroxybenzophenone, Zn, $TiCl_4$, THF; (b) NaH, MOMCl, THF; (c) NBS, CCl_4; (d) KCN, THF, H_2O; (e) methanol, HCl; (f) NaH, imidazole, THF; (g) NaH, 1,2,4-triazole, THF.

Analogues **17a**, **18a**, **19a** and **20a** were designed by incorporating a hydroxyl group on the "A" ring to probe the importance of a hydrogen bond donor in the para position. For analogues

17b, **18b**, **19b** and **20b**, a fluorine atom was introduced ortho to the "A" ring hydroxy group. The presence of the electronegative fluorine atom would increase the acidity of the hydroxy group and enable stronger hydrogen bonds to be formed. To prepare analogues **17-20**, the corresponding hydroxylated acetophenones **14a-b** were first protected with a pivaloyl group and the product reacted with 4,4'-dihydroxybenzophenone under the McMurry cross-coupling conditions to provide the bisphenols **15a-b** (Scheme 2). The phenolic hydroxyl groups were protected by MOM groups to afford **16a-b**. Compounds **16a-b** were brominated with NBS, followed by alkylation of KCN, to install the nitrile group. Unexpectedly, the pivaloyl group was also cleaved under the alkylation reaction conditions. In the next step, the MOM protecting groups were removed with HCl to directly provide the products **17a-b**. To prepare the imidazole products **18a-b**, compounds **16a-b** underwent a series of sequential reactions including bromination with NBS, alkylation of imidazole, deprotection of the pivaloyl group with KOH and removal of the MOM groups under acidic conditions to afford **18a-b** in good yield. Interestingly, subjection of **16a-b** to a similar sequence of reactions incorporating 1,2,4-triazole instead of imidazole led to the production of two isomers in each case (i.e. **19a** and **20a** were obtained from **16a**, and **19b** and **20b** were obtained from **16b**) due to the presence of two nonequivalent nucleophilic nitrogens in the 1,2,4-triazole system vs. only one for the imidazole case. Compounds **19a** and **19b** were isolated as the major products, and compounds **20a** and **20b** were the minor products.

Scheme 2. Synthesis of Analogues 17-20[a]

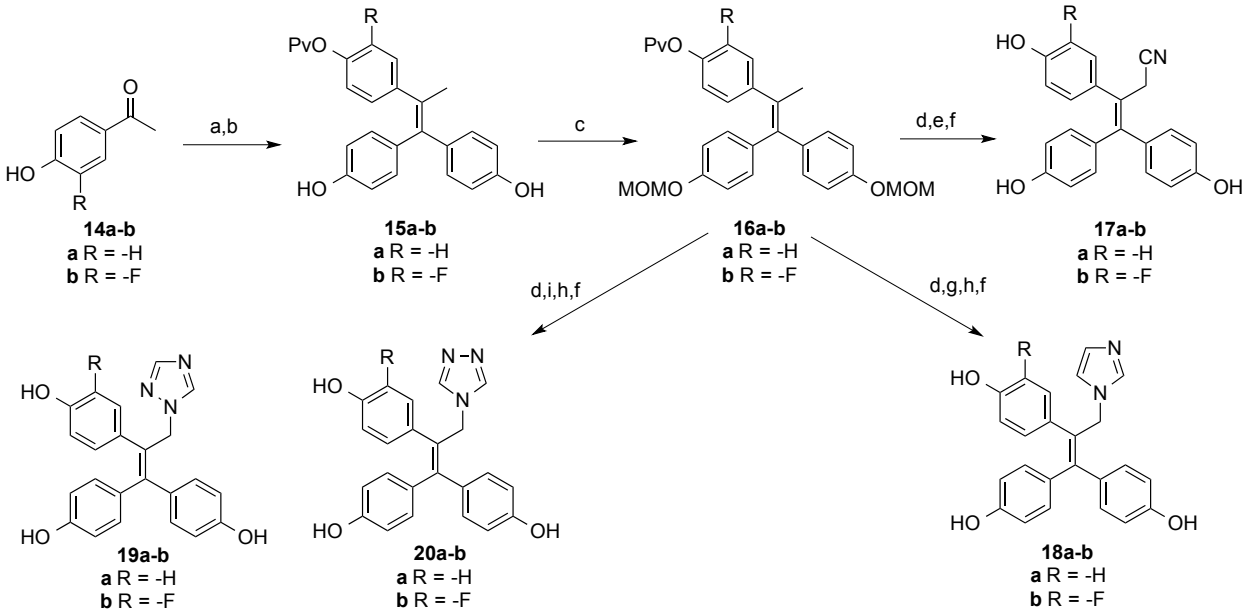

[a]Reagents and conditions: (a) NaH, PvCl, THF; (b) 4,4'-dihydroxybenzophenone, Zn, $TiCl_4$, THF; (c) NaH, MOMCl, THF; (d) NBS, CCl_4; (e) KCN, THF, H_2O; (f) methanol, HCl; (g) NaH, imidazole, THF; (h) KOH, THF, H_2O; (i) NaH, 1,2,4-triazole, THF.

In order to prepare analogues with an amino group in the para position of the "A" ring, 4-aminoacetophenone (**21**) was reacted with the di-protected 4,4'-dihydroxybenzophenone **22** under McMurry cross-coupling reaction conditions to afford **23** (Scheme 3). The amino group was protected with a Boc group, and the product **24** was subjected to a series of sequential reactions, including bromination with NBS, alkylation of KCN (both pivaloyl groups were cleaved under these conditions) and removal of the Boc group with HCl to afford the product **25** in very good yield. The imidazole product **26** and triazole products **27** and **28** were also obtained by subjecting **24** to a similar set of reactions.

Scheme 3. Synthesis of Analogues 25-28[a]

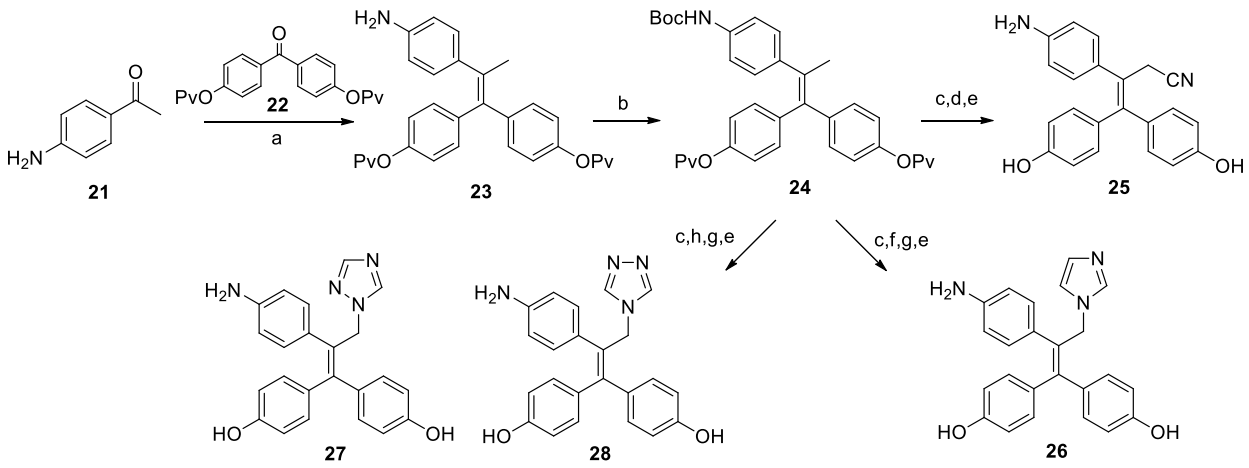

[a]Reagents and conditions: (a) Zn, $TiCl_4$, THF; (b) Boc_2O, dioxanes; (c) NBS, CCl_4; (d) KCN, H_2O, THF; (e) HCl, methanol; (f) NaH, imidazole, THF; (g) KOH, H_2O, THF; (h) NaH, 1,2,4-triazole, THF.

Analogue **32** was designed to probe the effect of introducing a hydroxyl group in the meta position of the "A" ring. The synthesis of **32** is outlined in Scheme 4. The phenolic hydroxyl group of **29** was first protected with a pivaloyl group. The product **30** reacted with 4,4'-dihydroxybenzophenone under McMurry cross-coupling reaction conditions, followed by protection of the phenolic hydroxyl groups with MOMCl, to afford **31**. Compound **31** underwent bromination with NBS, alkylation of imidazole, and removal of the pivaloyl group and MOM groups to afford **32** in good yield.

Scheme 4. Synthesis of Analogue 32[a]

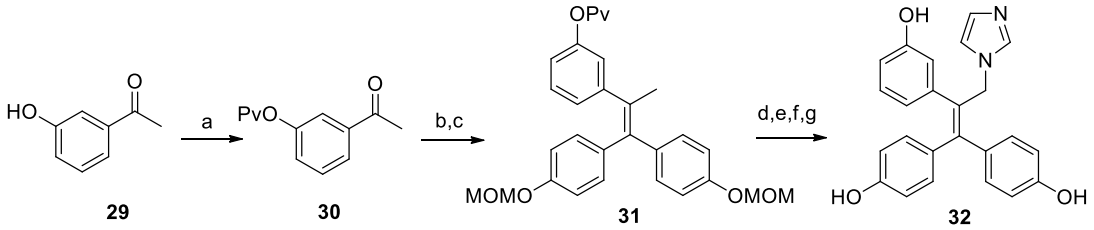

[a]Reagents and conditions: (a) NaH, PvCl, THF; (b) 4,4'-dihydroxybenzophenone, Zn, $TiCl_4$, THF; (c) NaH, MOMCl, THF; (d) NBS, CCl_4; (e) NaH, imidazole, THF; (f) KOH, H_2O, methanol; (g) HCl, methanol.

To synthesize analogue **35** with a meta amino group in the "A" ring, 3-aminoacetophenone (**33**) was reacted with the di-protected 4,4'-dihydroxybenzophenone **22** under McMurry cross-coupling reaction conditions, followed by protection of the amino group with a Boc group to afford **34** (in Scheme 5). Then, compound **34** underwent bromination with NBS, alkylation with imidazole and cleavage of the pivaloyl group and Boc group to provide **35** in good yield.

Scheme 5. Synthesis of Analogue 35[a]

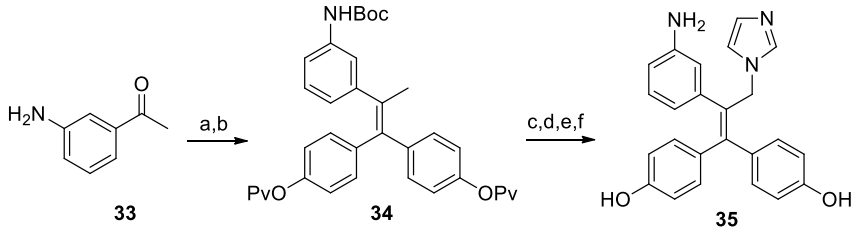

[a]Reagents and conditions: (a) **22**, Zn, $TiCl_4$, THF; (b) Boc_2O, dioxanes; (c) NBS, CCl_4; (d) NaH, imidazole, THF; (e) KOH, H_2O, methanol; (f) HCl, methanol.

Biological Activities. The aromatase inhibitory activities and ER-α/ER-β binding affinities of the bisphenols are summarized in Table 1. Compound **11** with a nitrile side chain showed slightly improved aromatase inhibitory activity (IC_{50} 12800 nM) when compared with compound **7** (IC_{50} 24900 nM), but it only displayed very weak binding affinity for both ER-α and ER-β. The imidazole compound **12** was the most potent aromatase inhibitor (IC_{50} 4.77 nM) and it also retained high binding affinities with both ER-α (EC_{50} 27.3 nM) and ER-β (EC_{50} 40.9 nM). Compound **13** with the triazole side chain was also a good aromatase inhibitor (IC_{50} 137 nM) but had weak ER binding affinity. Similar structure-activity relationships were also observed for compound series **17a-20a** and series **17b-20b**. The nitrile compounds (**17a** and **17b**) are weak aromatase inhibitors (IC_{50} 15200-17200 nM), and they showed no binding affinity for ER-α and ER-β. The triazole compounds (**19a-b** and **20a-b**) are moderate aromatase inhibitors (IC_{50} 2980-14200 nM), but they only showed weak binding affinities for ER-α ($EC_{50} \geq 943$ nM) and ER-β ($EC_{50} \geq 1080$ nM). The imidazole compounds (**18a** and **18b**) are very potent aromatase inhibitors (IC_{50} 60.0-94.4 nM), and they also displayed good binding affinities for ER-α (IC_{50} 85.2-97.8 nM) and ER-β (IC_{50} 56.3-73.6 nM). Compared with the "A" ring unsubstituted analogues **11-13**, introducing a hydroxyl group in the para position of the "A" ring (analogues **17a-20a**) unexpectedly resulted in moderate decreases in aromatase inhibitory activity or ER binding affinities. A comparison of series **17b-20b** with series **17a-20a** reveals that incorporating a fluorine atom ortho to the hydroxyl group produced minor effects on aromatase inhibitory activity and ER-α/ER-β binding affinity, except in the case of the two triazole systems it significantly decreased ER-α/ER-β affinity. The introduction of an amino group in the para position of the "A" ring (analogues **25-28**) either produced minor effects on aromatase inhibitory activity, or in the case of the nitriles **11** vs. **25**, it increased the inhibitory activity dramatically

(IC_{50} 12,800 vs. 36.3 nM). However, the para amino group is uniformly unfavorable for ER binding affinity. The imidazole **26** displayed much weaker binding affinities with ER-α (EC_{50} 1830 nM) and ER-β (EC_{50} 296 nM) compared with compound **12**, while compounds **25**, **27** and **28** all have weak binding affinities with ER. Rotating the "A" ring para hydroxyl group to the meta position (**32** vs **18a**) did not influence aromatase inhibitory activity, but it decreased the binding affinities with ER-α and ER-β significantly. Rotating the "A" ring para amino group to the meta position (**35** vs **26**) decreased both aromatase inhibitory activity and ER binding affinities.

Table 1. The Aromatase Inhibitory Activity and Estrogen Receptor Binding Affinities of Triphenylethylene Bisphenols [a,b]

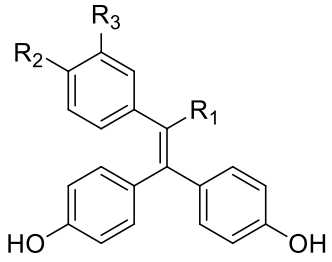

Cpd	R_1	R_2	R_3	Aromatase (IC_{50}, nM)	ER-α (EC_{50}, nM)	ER-β (EC_{50}, nM)
7	$-CH_2CH_3$	-H	-H	24900±1400	80% competition	307 ± 106
11	$-CH_2CN$	-H	-H	12800±2000	56% competition	49% competition
12		-H	-H	4.77 ± 0.38	27.3 ± 5.2	40.9 ± 12.1
13		-H	-H	137 ± 6	12% competition	33% competition
17a	$-CH_2CN$	-OH	-H	15200±300	0% competition	3% competition
18a		-OH	-H	60.0 ± 4.1	97.8 ± 42.3	73.6 ± 29.9
19a		-OH	-H	3030 ± 150	45% competition	40% competition
20a		-OH	-H	12500±400	943 ± 285	1080 ± 100
17b	$-CH_2CN$	-OH	-F	17200±2200	0% competition	0% competition
18b		-OH	-F	94.4 ± 3.5	85.2 ± 14.2	56.3 ± 17.8
19b		-OH	-F	2980 ± 50	2% competition	0% competition
20b		-OH	-F	14200±1100	0% competition	0% competition
25	$-CH_2CN$	$-NH_2$	-H	36.3 ± 0.8	0% competition	0% competition
26		$-NH_2$	-H	5.24 ± 0.41	1830 ± 910	296 ± 154
27		$-NH_2$	-H	104 ± 9	0% competition	2% competition
28		$-NH_2$	-H	17.7 ± 1.2	13% competition	36% competition
32		-H	-OH	60.4 ± 1.7	0% competition	29% competition
35		-H	$-NH_2$	439 ± 16	60% competition	71% competition

[a]The values are mean values of at least three experiments. [b]Percent ER competition was determined at the concentration of 100 μM for each compound. EC_{50} values were determined only for compounds that displayed > 90% competition.

Transcriptional Activities in MCF-7 Human Breast Cancer Cells. To investigate the effects of ligand binding on ER-mediated transcriptional activities, the triphenylethylene bisphenols were tested for their abilities to antagonize β–estradiol (E2) in a functional assay. Four compounds (**12**, **18a**, **18b** and **26**) were selected for this test because of their high binding affinities to both ER-α and ER-β. In this commonly used assay, the progesterone receptor (PGR) mRNA expression is used for assessing estrogenic or antiestrogenic activity in MCF-7 human breast cancer cells.[32] As shown in Figure 4, E2 (10 nM) was able to significantly increase the PGR mRNA expression compared to the control, which contained only 0.1% methanol (vehicle). The PGR mRNA expression level with 10 nM E2 stimulation alone was set as 100%, and the antiestrogenic effects of the compounds was monitored by the reduction of -stimulated mRNA levels. Endoxifen (positive control) can antagonize the PGR mRNA expression in the presence of 10 nM E2 to 10%, which is consistent with the published result.[32] (*E,Z*)-Norendoxifen can also antagonize the stimulatory effects of E2 as PGR mRNA expression level was reduced to 33% as we previously reported.[25] All of the tested triphenylethylene bisphenol analogues (**12**, **18a**, **18b** and **26**) were able to antagonize the ER-stimulated PGR mRNA expression to the levels of 26-31%, regardless of their different binding affinities with estrogen receptors. The antiestrogenic effects of the tested compounds as monitored by the reduction of estradiol-stimulated mRNA levels were weaker than endoxifen, but very similar to (*E,Z*)-norendoxifen.

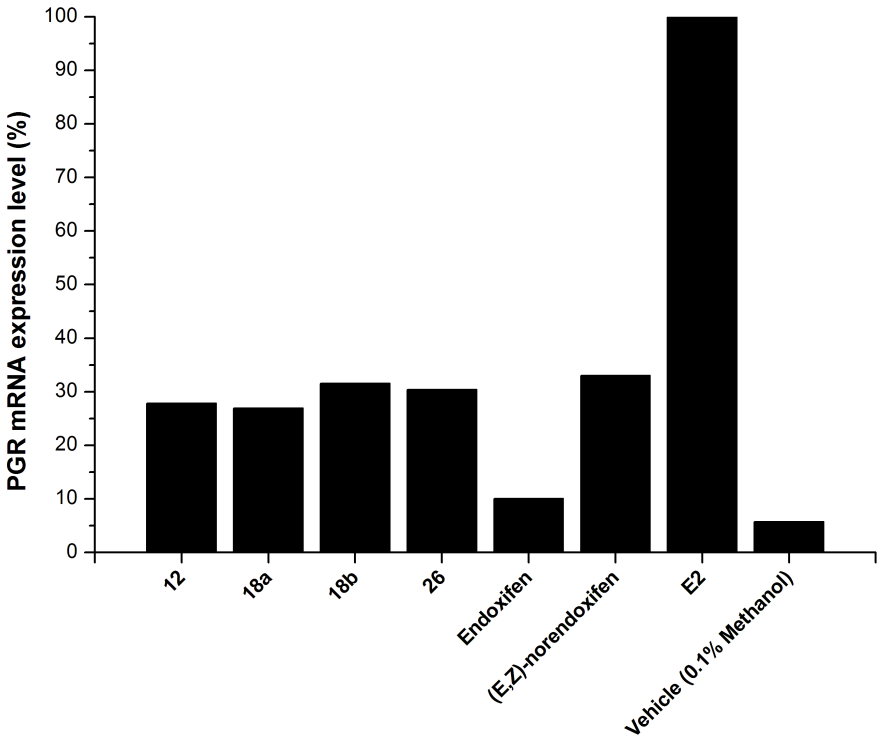

Figure 4. The abilities of compound **12**, **18a**, **18b** and **26** (1 μM) to antagonize β-estradiol (E2, 10 nM)-stimulated progesterone receptor (PGR) mRNA expression in MCF-7 cells.

Molecular Modeling. Molecular docking studies were performed in order to investigate the possible binding mode of the triphenylethylene bisphenol analogues with aromatase and ER-α. Compound **12** was docked into the active site of aromatase (PDB code: 3s79)[33] with GOLD 3.0. The high potency of **12** compared with **7** (> 5000 fold improvement in aromatase inhibitory activity) indicates imidazole-iron bonding. Therefore, a distance constraint (1.5-3.5 Å) was imposed between the imidazole nitrogen and iron during docking. The best docking pose of **12** (shown in Figure 5a) was overlapped with the hypothetical binding mode of *E*-norendoxifen (***E*-5**) that was previously reported (please see Supporting Information for more detailed molecular modeling results, including stereoviews, hydrogen bond angles, and distances calculated between

hydrogens and hydrogen bond acceptors).[24] The binding mode of **12** is in general very similar to that of *E*-norendoxifen, a result that is not surprising since the imidazole fragment was installed in **12** in a location for iron binding based on the structure calculated for the *E*-norendoxifen-aromatase complex. The imidazole group faces toward the heme and coordinates with the iron. One of the phenolic hydroxy groups forms a hydrogen bond with the backbone carbonyl group of Leu372, which is similar to *E*-norendoxifen binding. A notable difference between **12** and *E*-norendoxifen can be observed in their interaction with Ser478 and Asp309. For *E*-norendoxifen, a hydrogen bond was observed between the ether oxygen and the side chain hydroxyl group Ser478. For compound **12**, because of the size of the imidazole group the whole molecule moves "up" (further away from the heme) when compared with *E*-norendoxifen. Due to this move, the other phenolic hydroxy group moves away from Ser478 and approaches Asp309 with the formation of a hydrogen bond with the backbone carbonyl group of Asp309.

To explore the binding mode with ER-α, compound **12** was docked into the active site of ER-α (PDB code: 3ert)[34] with GOLD 3.0. The best docking pose of **12** (shown in Figure 5b) was overlapped with the published hypothetical binding mode of *Z*-norendoxifen (***Z*-5**). According to the docking results, the binding mode of **12** is nearly identical to that of *Z*-norendoxifen. The imidazole group is situated in the ethyl binding pocket surround by Met421, Met388 and Leu428. One of the phenolic hydroxy groups forms bifurcated hydrogen bonds with Arg394 and Glu353. The other phenolic hydroxy group projects toward the outside of the ligand binding pocket and forms a hydrogen bond with Thr347.

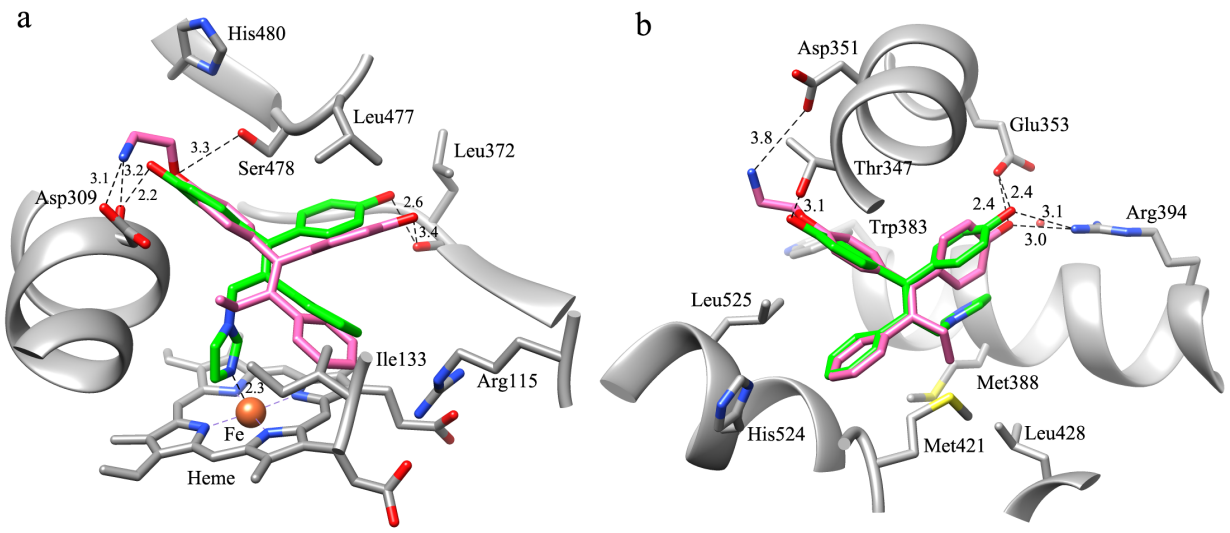

Figure 5. (a) The hypothetical binding mode of **12** (green) in the active site of aromatase (PDB code: 3s79)[33] overlapped with *E*-norendoxifen (pink). (b) The hypothetical binding mode of **12** (green) in the active site of ER-α (PDB code: 3ert)[34] overlapped with and *Z*-norendoxifen (pink).

Our previous testing results showed that the aminoethoxyl side chain of (*E,Z*)-norendoxifen (**5**) is favorable for aromatase inhibitory activity (>240 fold increase compared with **7**, Figure 6).[24] In this report, the imidazole group of compound **12** is also demonstrated to be optimal for aromatase inhibitory activity (>5000 fold increase compared with **7**). Unfortunately, combining the aminoethoxyl side chain and imidazole group in one molecule (compound **36**) did not result in a more potent aromatase inhibitor than **12**.[26] The failure of combining optimal substitutions to afford the most potent compound can be attributed to the hypothetical imidazole-induced binding mode movement as noted for compound **12**. The hypothetical binding mode of compound **36** overlapped with the hypothetical binding mode of *E*-norendoxifen (***E*-5**) is shown in Figure 6. Similar to compound **12**, the imidazole nitrogen of **36** coordinates with the iron. Because of the size of the imidazole group, the whole molecule **36** also moves "up" (further away from the

heme) when compared with *E*-norendoxifen. This movement pushes the ether oxygen away from Ser478 (distance 3.7 Å vs 3.3 Å of *E*-norendoxifen) and weakens the hydrogen bond between the ether oxygen and the side chain of Ser478. This movement also pushes the aminoethoxy side chain away from Asp309, resulting in the loss of the salt bridge interaction (between the protonated amino group and the carboxyl group of Asp309) and hydrogen bond (between the protonated amino group and the backbone carbonyl group of Asp309). Therefore, the aminoethoxy side chain of compound **36** cannot contribute positively to the aromatase inhibitory activity.

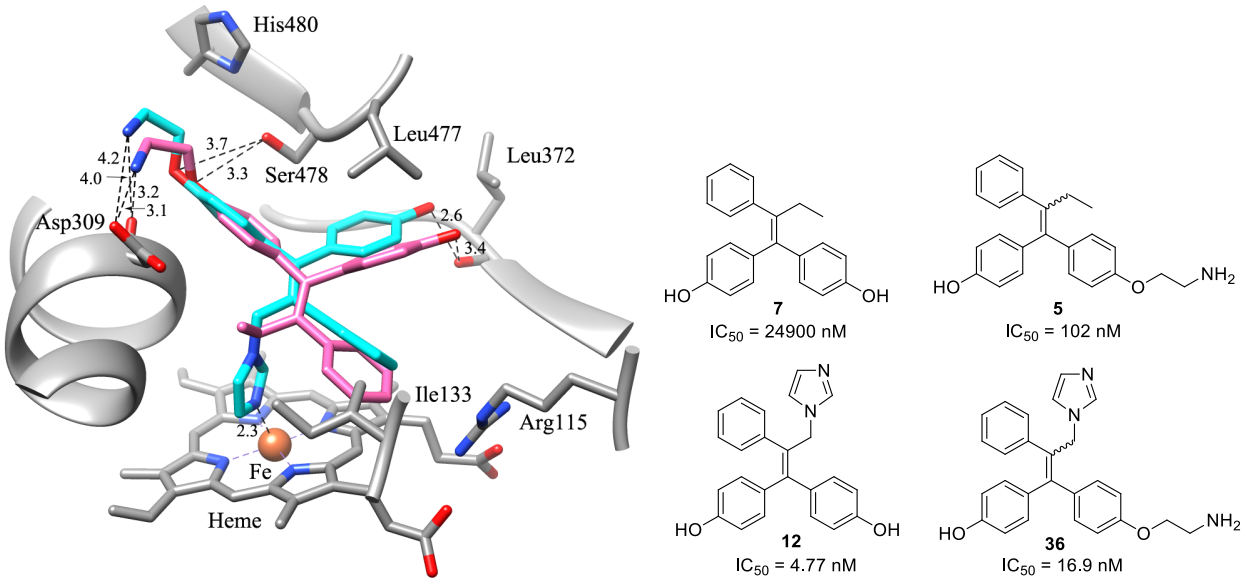

Figure 6. The hypothetical binding mode of compound **36** (cyan) in the active site of aromatase (PDB code: 3s79)[33] overlapped with *E*-norendoxifen (pink), and the comparison of aromatase inhibitory activities of compound **7**, **5**, **12** and **36**.

Conclusion

A series of triphenylethylene bisphenol analogues were designed and synthesized by eliminating the aminoethoxy side chain of (*E,Z*)-norendoxifen. The biological testing results showed that an imidazole group in the location of the ethyl group was optimal for both aromatase inhibitory activity and ER binding affinities. The imidazole compounds **12**, **18a**, **18b**, and **26** displayed superior aromatase inhibitory activity compared with (*E,Z*)-norendoxifen, while **12** also showed ER binding affinities comparable with (*E,Z*)-norendoxifen and **18a** and **18b** were slightly less active. These four imidazoles also act as antagonists in the ER transcriptional assays in MCF-7 breast cancer cells with activity similar to (*E,Z*)-norendoxifen. The possible binding modes of the most potent compound **12** with aromatase and ER-α were also investigated by molecular modeling and the results were used to rationalize the observed activity trends. Since these triphenylethylene bisphenol analogues have no possibility for the E/Z isomerization problems encountered with the norendoxifen analogues that were previously published, they introduce a superior class of compounds that can be developed toward the goal of obtaining therapeutically useful dual AI/SERM agents. Any future biological work with these compounds should provide a detailed profile of their agonistic and antagonistic activities in various organs and tissues in animal models. The facts that compound **12**, along with **18a** and **18b**, have high binding affinity to ER-α and ER-β and are analogues of the SERM tamoxifen argue in favor of the possibility of them being estrogen antagonists in breast tissue and estrogenic agonists in other tissues.

Experimental Section

General. Melting points were determined using capillary tubes with a Mel-Temp apparatus and are uncorrected. The nuclear magnetic resonance (^{1}H and ^{13}C NMR) spectra were recorded using a Bruker ARX300 spectrometer (300 MHz) with a QNP probe or a Bruker DRX-2 spectrometer (500 MHz) with a BBO probe. High-resolution mass spectra were recorded on a double-focusing sector mass spectrometer with magnetic and electrostatic mass analyzers. The purities of biologically important compounds are determined by HPLC or elemental analyses. For elemental analyses, the observed percentages differ less than 0.40% from the calculated values. For HPLC, the major peak accounted for $\geqslant$95% of the combined total peak area when monitored by a UV detector at 254 nm. The HPLC analyses were performed on a Waters 1525 binary HPLC pump/Waters 2487 dual λ absorbance detector system using a 5 μm C18 reversed phase column. The cytochrome P450 (CYP) inhibitor screening kit for aromatase (CYP19) was purchased from BD Biosciences (San Jose, CA). Estrogen receptor α and β competitor assay kits were purchased from Invitrogen (Carlsbad, CA).

General Procedure for the McMurry Cross-Coupling Reaction. Zinc powder (653 mg, 10 mmol) was suspended in dry THF (8 mL), the mixture was cooled to 0 ^{o}C, and then $TiCl_4$ (0.55 mL, 5 mmol) was added dropwise under argon. When the addition was complete, the mixture was warmed to room temperature and then heated at reflux for 2 h. After cooling down, a solution of the corresponding benzophenone (1 mmol) and ketone (3 mmol) in dry THF (8 mL) was added, and the mixture was heated at reflux in the dark for 3 h. After being cooled to room temperature, THF was evaporated. The residue was dissolved in saturated NH_4Cl aqueous solution (20 mL) and extracted with ethyl acetate (20 mL X 4). The organic layers were

combined, dried over Na_2SO_4, concentrated in vacuo and further purified by silica gel column chromatography to provide the McMurry cross-coupling product.

4-(1,1-Bis(4-hydroxyphenyl)prop-1-en-2-yl)phenyl Pivalate (15a). A suspension of **14a** (678 mg, 4.98 mmol) and NaH (206 mg, 95%, 8.15 mmol) in dry THF (5 mL) was stirred under argon for 10 min, and then pivaloyl chloride (0.90 mL, 7.31 mmol) was added. The solution was stirred at room temperature for 3 h and quenched with water (2 mL). The solvent was evaporated, and the residue was dissolved with water (15 mL) and extracted with ethyl acetate (15 mL X 4). The organic layers were combined, dried over Na_2SO_4, and concentrated. The concentrated product was reacted with 4,4'-dihydroxylbenzophenone (1.98 g, 9.24 mmol) according to the general McMurry cross coupling reaction procedure. The product was purified by silica gel column chromatography (2:1 hexanes-ethyl acetate) to afford the product **15a** as a white solid (1.55 g, 77%): mp 138-140 ^{o}C. ^{1}H NMR (300 MHz, methanol-d_4 and $CDCl_3$) δ 7.11-7.08 (m, 2 H), 7.03-7.00 (m, 2 H), 6.80-6.74 (m, 4 H), 6.69-6.66 (m, 2 H), 6.48-6.45 (m, 2 H), 2.07 (s, 3 H), 1.29 (s, 9 H); ^{13}C NMR (75 MHz, methanol-d_4 and $CDCl_3$) δ 179.3, 156.7, 156.0, 150.1, 143.7, 140.7, 136.6, 136.3, 134.0, 133.5, 132.6, 131.7, 122.1, 116.1, 115.6, 40.4, 28.3, 24.5; ESIMS *m/z* (relative intensity) 425 (MNa^+, 100); HRESIMS *m/z* calcd for $C_{26}H_{27}O_4$ (MH^+) 403.1909, found 403.1916.

4-(1,1-Bis(4-hydroxyphenyl)prop-1-en-2-yl)-2-fluorophenyl Pivalate (15b). A suspension of **14b** (187 mg, 1.21 mmol) and NaH (70.7 mg, 95%, 2.42 mmol) in dry THF (5 mL) was stirred at room temperature under argon. Pivaloyl chloride (0.22 mL, 1.8 mmol) was added dropwise. The mixture was stirred at room temperature for 3 h and quenched with water (2 mL). The THF was evaporated, and the residue was dissolved with 20% K_2CO_3 solution (20 mL) and extracted with ethyl acetate (15 mL X 3). The organic layers were combined and dried over

Na_2SO_4 and concentrated. The residue was combined with 4 4'- dihydroxybenzophenone (0.80 g, 3.73 mmol) and reacted according to the general McMurry cross-coupling reaction procedure. The product was further purified by silica gel column chromatography (7:3 hexanes-ethyl acetate) to afford the product **15b** as yellow oil (348 mg, 68%). ^{1}H NMR (300 MHz, $CDCl_3$) δ 7.07-7.04 (m, 2 H), 7.04-6.84 (m, 3 H), 6.79-6.76 (m, 2 H), 6.74-6.71 (m, 2 H), 6.52-6.49 (m, 2 H), 2.09 (s, 3 H), 1.35 (s, 9 H); EIMS *m/z* (relative intensity) 420 (M^+, 16), 57 (100); negative ion HRESIMS *m/z* calcd for $C_{26}H_{24}FO_4$ $(M - H^+)^-$ 419.1659, found 419.1665.

(2-(4-Aminophenyl)prop-1-ene-1,1-diyl)bis(4,1-phenylene) Bis(2,2-dimethylpropanoate) (23). Zinc powder (1.12 g, 17.1 mmol) was suspended in dry THF (10 mL) and the mixture was cooled to 0 ^{o}C. $TiCl_4$ (0.8 mL, 7.2 mmol) was added dropwise under argon. When the addition was complete, the mixture was warmed to room temperature and then heated at reflux for 2 h. After cooling down, a solution of **22**[35] (501 mg, 1.31 mmol) and **21** (175 mg, 1.29 mmol) in dry THF (10 mL) was added, and the mixture was heated at reflux in the dark for 3 h. After the reaction mixture was cooled to room temperature, THF was carefully evaporated. The residue was dissolved with saturated ammonium chloride aqueous solution (20 mL) and extracted with ethyl acetate (20 mL X 4). The organic layers were combined, dried over Na_2SO_4, concentrated in vacuo and further purified by silica gel column chromatography, eluting with 3:1 dichloromethane-hexanes, followed by 2:1 hexanes-ethyl acetate, to afford the product **23** as yellow solid (284 mg, 45%): mp 208-210 ^{o}C. ^{1}H NMR (300 MHz, $CDCl_3$) δ 7.23-7.20 (m, 2 H), 7.05-7.02 (m, 2 H), 6.95-6.92 (m, 2 H), 6.91-6.88 (m, 2 H), 6.76-6.73 (m, 2 H), 6.51-6.48 (m, 2 H), 2.10 (s, 3 H), 1.37 (s, 9 H), 1.31 (s, 9 H); ^{13}C NMR (75 MHz, $CDCl_3$) δ 177.1, 176.9, 149.5, 148.8, 144.8, 141.1, 140.7, 136.2, 136.1, 133.6, 131.8, 131.1, 130.3, 121.0, 120.4, 114.6,

39.1, 39.0, 27.1, 27.0, 23.3; ESIMS *m/z* (relative intensity) 508 (MNa^+, 100); HRESIMS *m/z* calcd for $C_{31}H_{36}NO_4$ (MH^+) 486.2645, found 486.2648.

General Procedure for the Preparation of 10 and 16a-b. A solution of bisphenol (**9** or **15a-b**, 0.502 mmol) and NaH (53.0 mg, 95%, 2.10 mmol) in dry THF (5 mL) was stirred under argon for 10 min, and then methyl chloromethyl ether (0.16 mL, 2.10 mmol) was added. The mixture was stirred at room temperature for 3 h and quenched with saturated aqueous $NaHCO_3$ solution (2 mL). The solvent was evaporated, and the residue was dissolved in saturated aqueous $NaHCO_3$ solution (15 mL) and extracted with ethyl acetate (15 mL X 4). The organic layers were combined, dried over Na_2SO_4, and concentrated in vacuo to provide the crude product **10** or **16a-b**.

4,4'-(2-Phenylprop-1-ene-1,1-diyl)bis((methoxymethoxy)benzene) (10). The crude product was purified by silica gel column chromatography (9:1 hexanes-ethyl acetate) to provide the pure product **10** as a colorless oil (69%). ^{1}H NMR (300 MHz, $CDCl_3$) δ 7.18-7.07 (m, 7 H), 7.04-7.00 (m, 2 H), 6.82-6.79 (m, 2 H), 6.71-6.68 (m, 2 H), 5.21 (s, 2 H), 5.07 (s, 2 H), 3.52 (s, 3 H), 3.43 (s, 3 H), 2.14 (s, 3 H); ^{13}C NMR (75 MHz, $CDCl_3$) δ 155.9, 155.2, 144.3, 138.2, 137.3, 136.9, 134.7, 132.0, 131.2, 129.3, 127.9, 126.0, 115.7, 115.0, 94.4, 94.3, 56.0, 55.9, 23.4; ESIMS *m/z* (relative intensity) 413 (MNa^+, 100); HRESIMS *m/z* calcd for $C_{25}H_{26}O_4Na$ (MNa^+) 413.1729, found 413.1731.

4-(1,1-Bis(4-(methoxymethoxy)phenyl)prop-1-en-2-yl)phenyl Pivalate (16a). The crude product was purified by silica gel column chromatography (85:15 hexanes-ethyl acetate) to provide the pure product **16a** as a colorless oil (81%). ^{1}H NMR (300 MHz, $CDCl_3$) δ 7.16-7.13 (m, 4 H), 7.02-6.99 (m, 2 H), 6.88-6.85 (m, 2 H), 6.82-6.79 (m, 2 H), 6.73-6.69 (m, 2 H), 5.19 (s, 2 H), 5.08 (s, 2 H), 3.51 (s, 3 H), 3.43 (s, 3 H), 2.12 (s, 3 H), 1.34 (s, 9 H); ^{13}C NMR (75 MHz,

$CDCl_3$) δ 177.0, 155.9, 155.3, 149.1, 141.6, 138.5, 137.2, 136.7, 133.8, 132.0, 131.1, 130.2, 120.8, 115.7, 115.2, 94.4, 56.0, 39.0, 27.1, 23.4; ESIMS *m/z* (relative intensity) 513 (MNa^+, 100); HRESIMS *m/z* calcd for $C_{30}H_{34}O_6Na$ (MNa^+) 513.2253, found 513.2272.

4-(1,1-Bis(4-(methoxymethoxy)phenyl)prop-1-en-2-yl)-2-fluorophenyl Pivalate (16b). The crude product was purified by silica gel column chromatography (85:15 hexanes-ethyl acetate) to provide the product **16b** as a colorless oil (194 mg, 49%). ^1H NMR (300 MHz, $CDCl_3$) δ 7.15-7.11 (m, 2 H), 7.02-6.99 (m, 2 H), 6.97-6.87 (m, 3 H), 6.82-6.79 (m, 2 H), 6.74-6.71 (m, 2 H), 5.19 (s, 2 H), 5.08 (s, 2 H), 3.50 (s, 3 H), 3.43 (s, 3 H), 2.10 (s, 3 H), 1.36 (s, 9 H); MALDIMS *m/z* (relative intensity) 508 (M^+, 80), 379 (100); HRESIMS *m/z* calcd for $C_{30}H_{33}FO_6Na$ (MNa^+) 531.2159, found 531.2143.

General Procedure for the Preparation of 11, 17a-b and 25. A solution of **10** or **16a-b** or **24** (0.169 mmol) and *N*-bromosuccinimide (30.8 mg, 0.173 mmol) in CCl_4 (5 mL) was heated at reflux under argon for 3 h. After cooling down, the solid was removed by filtration and the filtrate was concentrated in vacuo. The residue was dissolved in THF (4.5 mL) and a solution of KCN (46.2 mg, 0.709 mmol) in water (1.5 mL) was added. The mixture was stirred at room temperature overnight. The solvent was evaporated, and the residue was dissolved with water (10 mL) and extracted with ethyl acetate (10 mL X 3). The organic layers were combined, dried over Na_2SO_4, and concentrated in vacuo. The residue was dissolved with methanol (4.5 mL) and concentrated HCl (1 mL) was added. The solution was stirred at room temperature overnight. The solvent was removed, and the residue was dissolved with water (10 mL), neutralized with $NaHCO_3$, and extracted with ethyl acetate (10 mL X 3). The organic layers were combined, dried over Na_2SO_4, and concentrated in vacuo to provide the crude product **11** or **17a-b** or **25**.

4,4-Bis(4-hydroxyphenyl)-3-phenylbut-3-enenitrile (11). The crude product was purified by silica gel column chromatography (2:1 hexanes-ethyl acetate) to provide the pure product **11** as an orange solid (61.7 mg, 51%): mp 198-200 ^{o}C. ^{1}H NMR (300 MHz, methanol-d_4 and $CDCl_3$) δ 7.19-7.10 (m, 5 H), 7.09-7.05 (m, 2 H), 6.83-6.79 (m, 2 H), 6.69-6.65 (m, 2 H), 6.47-6.43 (m, 2 H), 3.50 (s, 2 H); ^{13}C NMR (75 MHz, methanol-d_4 and $CDCl_3$) δ 157.9, 157.0, 145.9, 141.5, 134.7, 134.3, 133.3, 132.1, 130.9, 129.7, 128.5, 127.2, 120.0, 116.8, 115.8, 26.8; EIMS *m/z* (relative intensity) 327 (M^+, 100); HREIMS *m/z* calcd for $C_{22}H_{17}NO_2$ (M^+) 327.1254, found 327.1264. Anal. Calcd for $C_{22}H_{17}NO_2 \cdot CH_3OH$: C, 76.86; H, 5.89; N, 3.90. Found: C, 76.88; H, 5.57; N, 3.93.

3,4,4-Tris(4-hydroxyphenyl)but-3-enenitrile (17a). The crude product **17a** was purified by silica gel column chromatography (1:1 hexanes-ethyl acetate) to provide the pure product as red foam (83%). ^{1}H NMR (300 MHz, methanol-d_4) δ 7.07-7.00 (m, 4 H), 6.84-6.80 (m, 2 H), 6.73-6.69 (m, 2 H), 6.66-6.62 (m, 2 H), 6.50-6.46 (m, 2 H), 3.53 (s, 2 H); ^{13}C NMR (75 MHz, methanol-d_4) δ 158.2, 157.6, 157.2, 144.5, 135.1, 134.8, 133.1, 132.7, 132.0, 131.8, 127.7, 120.1, 116.4, 116.2, 115.4, 25.8; ESIMS *m/z* (relative intensity) 366 (MNa^+, 100); HRESIMS *m/z* calcd for $C_{22}H_{17}NO_3Na$ (MNa^+) 366.1106, found 366.1120. HPLC purity 99.8% (C-18 reverse phase, methanol-H_2O, 90:10).

3-(3-Fluoro-4-hydroxyphenyl)-4,4-bis(4-hydroxyphenyl)but-3-enenitrile (17b). The crude product was purified by silica gel column chromatography (1:1 hexanes-ethyl acetate) to provide the pure product **17b** as white solid (70%): mp 180-183 ^{o}C. ^{1}H NMR (300 MHz, methanol-d_4) δ 7.07-7.04 (m, 2 H), 6.91-6.87 (m, 1 H), 6.84-6.79 (m, 3 H), 6.78-6.75 (m, 1 H), 6.73-6.70 (m, 2 H), 6.53-6.49 (m, 2 H), 3.55 (s, 2 H); EIMS *m/z* (relative intensity) 361 (M^+,

100); negative ion HRESIMS *m/z* calcd for $C_{22}H_{15}FNO_3$ $(M - H^+)^-$ 360.1036, found 360.1033. HPLC purity 99.3% (C-18 reverse phase, methanol-H_2O, 90:10).

3-(4-Aminophenyl)-4,4-bis(4-hydroxyphenyl)but-3-enenitrile (25). The crude product **25** was purified by silica gel column chromatography (1:1 hexanes-ethyl acetate) to provide the pure product **25** as white yellow solid (70%): mp 235-238 ^oC. ^1H NMR (300 MHz, methanol-d_4) δ 7.06-7.03 (m, 2 H), 6.96-6.93 (m, 2 H), 6.82-6.79 (m, 2 H), 6.72-6.69 (m, 2 H), 6.59-6.56 (m, 2 H), 6.47-6.44 (m, 2 H), 3.52 (s, 2 H); ^{13}C NMR (75 MHz, methanol-d_4) δ 158.1, 157.1, 147.9, 143.9, 135.3, 135.0, 133.1, 131.8, 131.6, 131.1, 128.0, 120.2, 116.4, 116.3, 115.3, 25.7; EIMS *m/z* (relative intensity) 342 (M^+, 100); HRESIMS *m/z* calcd for $C_{22}H_{19}N_2O_2$ (MH^+) 343.1447, found 343.1446. HPLC purity 97.8% (C-18 reverse phase, methanol-H_2O, 90:10).

General Procedure for the Preparation of 12 and 13. A solution of **10** (186 mg, 0.476 mmol) and *N*-bromosuccinimide (81.7 mg, 0.459 mmol) in CCl_4 (5 mL) was heated at reflux under argon for 3 h. After cooling down, the solid was removed by filtration and the filtrate was concentrated in vacuo. The residue was dissolved in dry THF (8 mL) and the solution was added to a solution of imidazole or 1,2,4-triazole (1.07 mmol) and NaH (30.1 mg, 1.25 mmol) in THF (4 mL) at 0 ^oC. The mixture was warmed to room temperature and stirred under argon overnight. The reaction was quenched with saturated NH_4Cl aqueous solution (1 mL). The solvent was evaporated, and the residue was dissolved with saturated NH_4Cl aqueous solution (25 mL) and extracted with ethyl acetate (25 mL X 4). The organic layers were combined, dried over Na_2SO_4, and concentrated in vacuo. The residue was dissolved with methanol (5 mL), concentrated HCl (0.4 mL), and heated at reflux for 0.5 h. The solvent was removed, and the residue was neutralized with saturated $NaHCO_3$ solution (15 mL) and extracted with ethyl acetate (15 mL X 4). The organic layers were combined, dried over Na_2SO_4, concentrated in vacuo and further

purified by silica gel column chromatography (95:5 dichloromethane-methanol) to provide the product **12** or **13**.

4,4'-(3-(1*H*-Imidazol-1-yl)-2-phenylprop-1-ene-1,1-diyl)diphenol (12). The purified product was dissolved in DMSO (1 mL) and then diluted with water (10 mL). The solid was collected by filtration and dried in vacuo to provide the product **12** as a yellow solid (150 mg, 89%): mp 225-227 ^{o}C. ^{1}H NMR (300 MHz, DMSO-d_6) δ 7.41 (s, 1 H), 7.10-6.99 (m, 8 H), 6.79-6.76 (m, 3 H), 6.69-6.66 (m, 2 H), 6.44-6.41 (m, 2 H), 4.89 (s, 2 H); ^{13}C NMR (75 MHz, DMSO-d_6) δ 157.6, 156.8, 144.8, 140.8, 133.6, 132.7, 132.3, 131.0, 130.4, 128.8, 127.4, 119.9, 116.2, 115.3, 51.1; ESIMS *m/z* (relative intensity) 369 (MH^+, 33), 301 (100); HRESIMS *m/z* calcd for $C_{24}H_{20}N_2O_2Na$ (MNa^+) 391.1422, found 391.1414. Anal. Calcd for $C_{24}H_{20}N_2O_2 \cdot 1.3\ H_2O$: C, 73.56; H, 5.81; N, 7.15. Found: C, 73.47; H, 5.83; N, 6.90.

4,4'-(2-Phenyl-3-(1*H*-1,2,4-triazol-1-yl)prop-1-ene-1,1-diyl)diphenol (13). Yellow solid (54 mg, 54%): mp 143-145 ^{o}C. ^{1}H NMR (300 MHz, methanol-d_4 and $CDCl_3$) δ 7.98 (s, 1 H), 7.90 (s, 1 H), 7.19-7.15 (m, 2 H), 7.08-7.02 (m, 5 H), 6.80-6.77 (m, 2 H), 6.73-6.69 (m, 2 H), 6.46-6.43 (m, 2 H), 5.20 (s, 2 H); ^{13}C NMR (75 MHz, methanol-d_4 and $CDCl_3$) δ 158.0, 157.1, 147.3, 140.9, 134.5, 133.4, 132.1, 130.8, 129.7, 128.2, 116.6, 115.7, 56.0; EIMS *m/z* (relative intensity) 369 (M^+, 53), 300 (100); HREIMS *m/z* calcd for $C_{23}H_{19}N_3O_2$ (M^+) 369.1472, found 369.1484. Anal. Calcd for $C_{23}H_{19}N_3O_2 \cdot 1.6\ CH_3OH$: C, 70.23; H, 6.09; N, 9.99. Found: C, 70.48; H, 5.70; N, 9.59.

General Procedure for the Preparation of 18a-b and 26. A solution of **16a-b** or **24** (0.127 mmol) and *N*-bromosuccinimide (24.8 mg, 0.139 mmol) in CCl_4 (5 mL) was heated at reflux under argon for 3 h. After cooling down, the solid was removed by filtration and the filtrate was concentrated in vacuo. The residue was dissolved in dry THF (5 mL) and the solution

was added to a solution of imidazole (35.4 mg, 0.52 mmol) and NaH (27.1 mg, 95%, 1.07 mmol) in THF (3 mL). The mixture was stirred at room temperature overnight. The reaction was quenched with saturated NH_4Cl aqueous solution (1 mL). The solvent was evaporated, and the residue was dissolved with saturated NH_4Cl aqueous solution (10 mL) and extracted with ethyl acetate (10 mL X 3). The organic layers were combined, dried over Na_2SO_4 and concentrated in vacuo. The product was dissolved in THF (2.5 mL) and 2 N KOH solution (2.5 mL) was added. The mixture was stirred at room temperature overnight. The solvent was evaporated, and the residue was dissolved with saturated NH_4Cl aqueous solution (15 mL) and extracted with ethyl acetate (10 mL X 3). The organic layers were combined, dried over Na_2SO_4, concentrated in vacuo and further purified by silica gel column chromatography (95:5 dichloromethane-methanol). The purified product was dissolved with methanol (4.5 mL) and concentrated HCl (1 mL) was added. The mixture was stirred at room temperature overnight. The solvent was evaporated, and the residue was dissolved with water (10 mL), neutralized with $NaHCO_3$, and extracted with ethyl acetate (10 mL X 3). The organic layers were combined, dried over Na_2SO_4, concentrated in vacuo and further purified by silica gel column chromatography (9:1 dichloromethane-methanol) to provide the product **18a-b** or **26.**

4,4',4''-(3-(1*H*-Imidazol-1-yl)prop-1-ene-1,1,2-triyl)triphenol (18a). Red glass (58%). ^{1}H NMR (300 MHz, methanol-d_4) δ 7.35 (s, 1 H), 7.06-7.03 (m, 2 H), 6.91 (s, 1 H), 6.88-6.79 (m, 5 H), 6.77-6.73 (m, 2 H), 6.58-6.54 (m, 2 H), 6.49-6.45 (m, 2 H), 4.88 (s, 2 H); ^{13}C NMR (75 MHz, methanol-d_4) δ 158.0, 157.3, 157.1, 145.2, 138.3, 134.9, 133.0, 132.4, 132.1, 131.7, 128.6, 120.5, 116.4, 116.1, 115.4, 52.2; negative ion ESIMS *m/z* (relative intensity) 383 [(M - H^+)$^-$, 8], 315 (100); negative ion HREIMS *m/z* calcd for $C_{24}H_{19}N_2O_3$ (M - H^+)$^-$ 383.1396, found 383.1398. HPLC purity 97.6% (C-18 reverse phase, methanol-H_2O, 90:10).

4,4'-(2-(3-Fluoro-4-hydroxyphenyl)-3-(1*H*-imidazol-1-yl)prop-1-ene-1,1-diyl)diphenol (18b). Orange foam (49%). ^{1}H NMR (300 MHz, methanol-d_4) δ 7.41 (s, 1 H), 7.08-7.05 (m, 2 H), 6.97 (s, 1 H), 6.85 (s, 1 H), 6.82-6.79 (s, 2 H), 6.77-6.74 (m, 2 H), 6.73-6.65 (m, 3 H), 6.51-6.48 (m, 2 H), 4.92 (s, 2 H); ESIMS *m/z* (relative intensity) 403 (MH^+, 13), 335 (100); HRESIMS *m/z* calcd for $C_{24}H_{20}FN_2O_3$ (MH^+) 403.1458, found 403.1459. HPLC purity 98.9% (C-18 reverse phase, methanol-H_2O, 90:10).

4,4'-(2-(4-Aminophenyl)-3-(1*H*-imidazol-1-yl)prop-1-ene-1,1-diyl)diphenol (26). Yellow foam (59%). ^{1}H NMR (300 MHz, methanol-d_4) δ 7.40 (s, 1 H), 7.05-7.01 (m, 2 H), 6.94 (s, 1 H), 6.84-6.73 (m, 7 H), 6.52-6.49 (m, 2 H), 6.47-6.43 (m, 2 H), 4.90 (s, 2 H); ^{13}C NMR (75 MHz, methanol-d_4) δ 158.0, 157.1, 147.6, 144.8, 138.2, 135.1, 133.2, 133.0, 131.7, 130.8, 128.3, 120.6, 116.3, 115.3, 52.2; ESIMS *m/z* (relative intensity) 384 (MH^+, 18), 316 (100); HRESIMS *m/z* calcd for $C_{24}H_{22}N_3O_2$ (MH^+) 384.1712, found 384.1725. HPLC purity 99.4% (C-18 reverse phase, methanol-H_2O, 90:10), 99.8% (C-18 reverse phase, methanol-H_2O, 85:15).

General Procedure for the Preparation of 19a-b, 20a-b, 27 and 28. A solution of **16a-b** or **24** (0.201 mmol) and *N*-bromosuccinimide (35.8 mg, 0.201 mmol) in CCl_4 (5 mL) was heated at reflux under argon for 3 h. After cooling down, the solid was removed by filtration and the filtrate was concentrated in vacuo. The residue was dissolved in dry THF (6 mL) and the solution was added to a solution of 1,2,4-triazole (42.6 mg, 0.62 mmol) and NaH (32 mg, 95%, 1.27 mmol) in THF (3 mL). The mixture was stirred at room temperature overnight. The reaction was quenched with saturated NH_4Cl aqueous solution (1 mL). The solvent was evaporated, and the residue was dissolved in saturated ammonium chloride aqueous solution (10 mL) and extracted with ethyl acetate (10 mL X 3). The organic layers were combined, dried over Na_2SO_4, and concentrated in vacuo. The product was dissolved in THF (2.5 mL) and 2 N KOH solution (2.5

mL) was added. The mixture was stirred at room temperature overnight. The solvent was evaporated, and the residue was dissolved with saturated aqueous ammonium chloride solution (15 mL) and extracted with ethyl acetate (10 mL X 3). The organic layers were combined, dried over Na_2SO_4, concentrated in vacuo and further purified by silica gel column chromatography (95:5 dichloromethane-methanol). The purified product was dissolved in methanol (4.5 mL) and concentrated HCl (1 mL) was added. The mixture was stirred at room temperature overnight. The solvent was evaporated, and the residue was dissolved in water (10 mL), neutralized with $NaHCO_3$, and extracted with ethyl acetate (10 mL X 3). The organic layers were combined, dried over Na_2SO_4, concentrated in vacuo and further purified by silica gel column chromatography (9:1 dichloromethane-methanol) to first provide **19a-b** or **27** and then **20a-b** or **28**.

4,4',4''-(3-(1*H*-1,2,4-Triazol-1-yl)prop-1-ene-1,1,2-triyl)triphenol (19a). Yellow oil (93.1 mg, 60%). ^{1}H NMR (300 MHz, methanol-d_4) δ 8.00 (s, 1 H), 7.87 (s, 1 H), 7.28-7.25 (m, 2 H), 6.90-6.87 (m, 2 H), 6.81-6.74 (m, 4 H), 6.55-6.52 (m, 2 H), 6.49-6.46 (m, 2 H), 5.18 (s, 2 H); ^{13}C NMR (75 MHz, methanol-d_4) δ 158.0, 157.3, 157.1, 151.8, 145.3, 135.2, 134.8, 133.2, 132.2, 132.1, 131.9, 116.2, 116.1, 115.4, 55.0; negative ion ESIMS *m/z* (relative intensity) 384 [(M - $H^+)^-$, 5], 315 (100); negative ion HREIMS *m/z* calcd for $C_{23}H_{18}N_3O_3$ [(M - $H^+)^-$] 384.1348, found 384.1353. HPLC purity 98.8% (C-18 reverse phase, methanol-H_2O, 90:10).

4,4',4''-(3-(4*H*-1,2,4-Triazol-4-yl)prop-1-ene-1,1,2-triyl)triphenol (20a). Yellow oil (32.5 mg, 21%). ^{1}H NMR (300 MHz, methanol-d_4) δ 8.23 (s, 2 H), 7.08-7.05 (m, 2 H), 6.95-6.92 (m, 2 H), 6.83-6.80 (m, 2 H), 6.78-6.75 (m, 2 H), 6.60-6.57 (m, 2 H), 6.48-6.45 (m, 2 H), 5.03 (s, 2 H); ^{13}C NMR (75 MHz, methanol-d_4) δ 158.2, 157.7, 157.4, 146.0, 144.5, 134.7, 134.5, 133.0, 132.1, 131.8, 131.5, 116.5, 116.4, 115.4, 50.8; negative ion ESIMS *m/z* (relative intensity) 384

[(M - H^+)$^-$, 3], 315 (100); negative ion HREIMS *m/z* calcd for $C_{23}H_{18}N_3O_3$ (M - H^+)$^-$ 384.1348, found 384.1359. HPLC purity 96.1% (C-18 reverse phase, methanol-H_2O, 90:10).

4,4'-(2-(3-Fluoro-4-hydroxyphenyl)-3-(1*H*-1,2,4-triazol-1-yl)prop-1-ene-1,1-diyl)diphenol (19b). Orange foam (37%). ^{1}H NMR (300 MHz, methanol-d_4) δ 8.07 (s, 1 H), 7.90 (s, 1 H), 7.29-7.26 (s, 2 H), 6.83-6.61 (m, 7 H), 6.52-6.47 (m, 2 H), 5.20 (s, 2 H); ESIMS *m/z* (relative intensity) 426 (MNa^+, 100); HRESIMS *m/z* calcd for $C_{23}H_{18}FN_3O_3Na$ (MNa^+) 426.1230, found 426.1243. HPLC purity 99.6% (C-18 reverse phase, methanol-H_2O, 90:10).

4,4'-(2-(3-Fluoro-4-hydroxyphenyl)-3-(4*H*-1,2,4-triazol-4-yl)prop-1-ene-1,1-diyl)diphenol (20b). Yellow foam (21%). ^{1}H NMR (300 MHz, methanol-d_4) δ 8.31 (s, 2 H), 7.11-7.06 (m, 2 H), 6.86-6.66 (m, 7 H), 6.53-6.49 (m, 2 H), 5.06 (s, 2 H); ESIMS *m/z* (relative intensity) 426 (MNa^+, 100); HRESIMS *m/z* calcd for $C_{23}H_{18}FN_3O_3Na$ (MNa^+) 426.1230, found 426.1244. HPLC purity 98.0% (C-18 reverse phase, methanol-H_2O, 90:10).

4,4'-(2-(4-Aminophenyl)-3-(1*H*-1,2,4-triazol-1-yl)prop-1-ene-1,1-diyl)diphenol (27). Orange foam (24%). ^{1}H NMR (300 MHz, methanol-d_4) δ 8.02 (s, 1 H), 7.87 (s, 1 H), 7.26-7.23 (m, 2 H), 6.85-6.82 (m, 2 H), 6.79-6.73 (m, 4 H), 6.50-6.43 (m, 4 H), 5.19 (s, 2 H); ^{13}C NMR (75 MHz, methanol-d_4) δ 158.0, 157.1, 151.7, 147.5, 145.2, 144.8, 135.4, 135.0, 133.1, 132.1, 131.7, 130.3, 116.3, 116.1, 115.3, 54.9; ESIMS *m/z* (relative intensity) 407 (MNa^+, 100); HRESIMS *m/z* calcd for $C_{23}H_{20}N_4O_2Na$ (MNa^+) 407.1484, found 407.1490. HPLC purity 97.6% (C-18 reverse phase, methanol-H_2O, 90:10).

4,4'-(2-(4-Aminophenyl)-3-(4*H*-1,2,4-triazol-4-yl)prop-1-ene-1,1-diyl)diphenol (28). Yellow foam (20%). ^{1}H NMR (300 MHz, methanol-d_4) δ 8.24 (s, 2 H), 7.06-7.03 (m, 2 H), 6.89-6.86 (m, 2 H), 6.83-6.80 (m, 2 H), 6.79-6.76 (m, 2 H), 6.54-6.51 (m, 2 H), 6.47-6.44 (m, 2 H), 5.03 (s, 2 H); ^{13}C NMR (75 MHz, methanol-d_4) δ 158.2, 157.3, 148.0, 145.4, 144.5, 134.9, 134.7,

133.0, 132.0, 131.7, 131.5, 129.7, 116.5, 116.4, 115.3, 50.8; ESIMS *m/z* (relative intensity) 407 (MNa^+, 100); HRESIMS *m/z* calcd for $C_{23}H_{20}N_4O_2Na$ (MNa^+) 407.1484, found 407.1498. HPLC purity 99.2% (C-18 reverse phase, methanol-H_2O, 90:10).

(2-(4-((*tert*-Butoxycarbonyl)amino)phenyl)prop-1-ene-1,1-diyl)bis(4,1-phenylene) Bis(2,2-dimethylpropanoate) (24). A solution of **23** (284 mg, 0.585 mmol) and Boc_2O (207 mg, 0.948 mmol) in dry dioxane (10 mL) was heated at reflux under argon for 5 h. After cooling down, the solvent was evaporated, and the residue was dissolved with 10% K_2CO_3 solution (20 mL) and exacted with ethyl acetate (20 mL X 3). The organic layers were combined, dried over Na_2SO_4, concentrated and further purified by silica gel column chromatography (85:15 hexanes-ethyl acetate) to provide **24** as white solid (274 mg, 80%): mp 187-190 ^oC. ^1H NMR (300 MHz, $CDCl_3$) δ 7.23-7.20 (m, 2 H), 7.18-7.15 (m, 2 H), 7.06-7.02 (m, 4 H), 6.89-6.86 (m, 2 H), 6.75-6.72 (m, 2 H), 2.10 (s, 3 H), 1.50 (s, 9 H), 1.36 (s, 9 H), 1.30 (s, 9 H); ^{13}C NMR (75 MHz, $CDCl_3$) δ 177.0, 176.9, 149.6, 149.0, 146.7, 140.7, 140.2, 138.1, 137.2, 136.6, 135.7, 131.8, 131.0, 129.8, 121.1, 120.4, 117.8, 80.4, 39.1, 39.0, 27.4, 27.1, 27.0, 23.3; EIMS *m/z* (relative intensity) 585 (M^+, 0.6), 57 (100); HRESIMS *m/z* calcd for $C_{36}H_{43}NO_6Na$ (MNa^+) 608.2988, found 608.3009.

3-Acetylphenyl Pivalate (30).[36] A solution of compound **29** (421 mg, 3.09 mmol) in dry THF (7 mL) was stirred under argon. NaH (111 mg, 95%, 4.39 mmol) was added portionwise. The solution was stirred for 30 min and then trimethylacetyl chloride (0.6 mL, 4.87 mmol) was added dropwise. After stirring for 2 h, the reaction was quenched with H_2O (2 mL) and the solvent was evaporated. The residue was dissolved with H_2O (20 mL) and extracted with ethyl acetate (3×10 mL). The organic layers were combined, dried over Na_2SO_4, concentrated in vacuo and further purified by silica gel chromatography (4:1 hexanes-ethyl acetate) to provide **30**

as pale yellow oil (541 mg, 95%). ^{1}H NMR (300 MHz, $CDCl_3$) δ 7.74 (d, *J* = 7.7 Hz, 1 H), 7.59 (s, 1 H), 7.40 (t, *J* = 7.9 Hz, 1 H), 7.21 (d, *J* = 8.1 Hz, 1 H), 2.53 (s, 3 H), 1.32 (s, 9 H).

3-(1,1-Bis(4-(methoxymethoxy)phenyl)prop-1-en-2-yl)phenyl Pivalate (31). The acetophenone **30** (1.47 g, 6.67 mmol) and 4,4'-dihydroxylbenzophenone (0.953 g, 4.4 mmol) were reacted according to the general McMurry cross-coupling reaction procedure. The product was purified by silica gel column chromatography (2:1 hexanes-ethyl acetate) to provide impure bisphenol intermediate which was dissolved in dry THF (20 mL) and treated with NaH (0.231 g, 95%, 9.14 mmol). The mixture was stirred 30 min under argon, and then chloromethyl methyl ether (2.0 mL, 9.0 mmol) was added dropwise. After stirring 3 h, the reaction was quenched with saturated $NaHCO_3$ (10 mL) and the solvent was evaporated. The organic products were extracted from the aqueous phase using ethyl acetate (3×15 mL). The organic layers were combined, dried over Na_2SO_4, concentrated and purified by silica gel column chromatography, eluting with 6:1 hexanes-ethyl acetate to provide product **31** as pale yellow oil (0.912 g, 43%). ^{1}H NMR (300 MHz, $CDCl_3$) δ 7.19-7.09 (m, 3 H), 7.06-7.00 (m, 2 H), 6.95 (dt, *J* = 7.7, 1.3 Hz, 1 H), 6.89 (t, *J* = 2.0 Hz, 1 H), 6.86-6.78 (m, 3 H), 6.76-6.71 (m, 2 H), 5.20 (s, 2 H), 5.08 (s, 2 H), 3.51 (s, 3 H), 3.43 (s, 3 H), 2.15 (s, 3 H), 1.34 (s, 9 H); ^{13}C NMR (75 MHz, $CDCl_3$) δ 176.92, 155.92, 155.45, 150.75, 145.63, 138.87, 137.06, 136.52, 133.56, 131.88, 131.09, 128.66, 126.78, 122.19, 119.07, 115.71, 115.18, 94.40, 55.91, 38.97, 27.08, 23.17; ESIMS *m/z* (MNa^+) 513; HRESIMS *m/z* cacld for $C_{30}H_{34}O_6$ (MNa^+) 513.2253, found 513.2234.

4,4'-(2-(3-Hydroxyphenyl)-3-(1*H*-imidazol-1-yl)prop-1-ene-1,1-diyl)diphenol (32). A solution of **31** (0.68 g, 1.39 mmol) and *N*-bromosuccinimide (247 mg, 1.39 mmol) in CCl_4 (30 mL) was heated at reflux under argon for 2 h. After cooling down, the solid was filtered off, and the solvent was evaporated. The residue was dissolved in dry THF (10 mL) and added to a

solution of NaH (67 mg, 95%, 2.78 mmol) and imidazole (143 mg, 2.1 mmol) in dry THF (10 mL). The mixture was stirred at room temperature overnight. The reaction was then quenched with saturated NH_4Cl (4 mL) solution and the solvent was evaporated. The product was extracted from saturated NH_4Cl (15 mL) solution using ethyl acetate (3×15 mL). The organic layers were combined, dried over Na_2SO_4 and concentrated. The product was dissolved in methanol (5 mL) and treated with 2 N KOH to bring the pH above 12. After the reaction mixture was stirred overnight, it was quenched with saturated NH_4Cl (10 mL) solution and the solvents were evaporated. The product was extracted from saturated NH_4Cl (10 mL) solution using ethyl acetate (4×10 mL). The organic layers were combined, dried over Na_2SO_4 and concentrated. The product was dissolved in methanol (10 mL) and treated with concentrated HCl (1 mL). After stirring overnight, the reaction was neutralized using $NaHCO_3$ and methanol was evaporated. Saturated NH_4Cl (10 mL) solution was added and the product was extracted using ethyl acetate (3×10 mL). The organic layers were combined, washed with brine, dried over Na_2SO_4, concentrated, and further purified using silica gel column chromatography, eluting with 10:1 dichloromethane-methanol to provide **32** (103 mg, 21%) as white glass. ^{1}H NMR (300 MHz, methanol-d_4) δ 7.35 (s, 1 H), 7.09-7.04 (m, 2 H), 7.01-6.90 (m, 2 H), 6.86-6.74 (m, 5 H), 6.56 (dd, J = 2.0, 1.1 Hz, 1 H), 6.52 (dq, J = 4.2, 1.6 Hz, 2 H), 6.49-6.43 (m, 2 H), 4.89 (s, 2 H); ^{13}C NMR (75 MHz, methanol-d_4) δ 160.80, 160.65, 159.84, 148.40, 145.46, 140.76, 137.12, 137.01, 135.68, 135.39, 134.14, 132.82, 131.11, 124.67, 123.00, 120.24, 118.87, 117.84, 117.40, 54.78; ESIMS *m/z* (relative intensity) 385 (MH^+, 16), 317 (100); HRESIMS *m/z* cacld for $C_{24}H_{20}N_2O_3$ (MH^+) 385.1552, found 385.1556. HPLC purity: 100% (C-18 reverse phase, methanol-H_2O, 90:10).

(2-(3-((*tert*-Butoxycarbonyl)amino)phenyl)prop-1-ene-1,1-diyl)bis(4,1-phenylene) Bis(2,2-dimethylpropanoate) (34). The acetophenone **33** (0.201 g, 1.49 mmol) and benzophenone **22** (0.682 g, 1.78 mmol) were reacted according to the general McMurry cross-coupling reaction procedure. The product was purified by silica gel chromatography (4:1 hexanes-ethyl acetate) to provide the impure intermediate, which was then treated with di-*tert*-butyl dicarbonate (0.312 g, 1.43 mmol) in THF (20 mL). The reaction mixture stirred under argon for 36 h. The solvent was evaporated and the residue was purified by silica gel chromatography (4:1 hexanes-ethyl acetate) to provide **34** as cloudy oil (0.685 g, 79%). ^{1}H NMR (300 MHz, $CDCl_3$) δ 7.25-7.13 (m, 4 H), 7.11-7.02 (m, 3 H), 6.92-6.86 (m, 2 H), 6.78 (s, 1 H), 6.76-6.71 (m, 2 H), 6.42 (brs, 1 H), 2.12 (s, 3 H), 1.51 (s, 9 H), 1.37 (s, 9 H), 1.30 (s, 9 H); ^{13}C NMR (75 MHz, $CDCl_3$) δ 177.01, 152.65, 149.69, 149.06, 144.51, 140.44, 139.98, 138.03, 137.55, 136.06, 131.65, 130.96, 128.56, 124.21, 121.09, 120.40, 119.08, 116.68, 80.31, 39.06, 28.31, 27.05, 23.42; HRESIMS *m/z* (relative intensity) calcd for $C_{36}H_{43}NO_6$ (MNa^+) 608.2988, found 608.2999.

4,4'-(2-(3-Aminophenyl)-3-(1*H*-imidazol-1-yl)prop-1-ene-1,1-diyl)diphenol (35). A solution of **34** (0.341 g, 0.58 mmol) and *N*-bromosuccinimide (83 mg, 0.46 mmol) in CCl_4 (30 mL) was heated at reflux under argon for 2 h. After cooling down, the solid was filtered off, and the solvent was evaporated. The residue was dissolved in dry THF (10 mL) and added to a solution of NaH (16 mg, 95%, 0.63 mmol) and imidazole (39 mg, 0.58 mmol) in dry THF (15 mL). The mixture was stirred at room temperature overnight. The reaction was then quenched with saturated NH_4Cl (3 mL) solution and the solvent was evaporated. The residue was dissolved in saturated NH_4Cl (10 mL) and the product was extracted using ethyl acetate (3×15 mL). The organic layers were combined, washed with brine (10 mL), dried over Na_2SO_4 and concentrated.

The product was dissolved in methanol-THF (7:3, 10 mL) and treated with 1 N KOH (2 mL). After the reaction mixture stirred 1 h, it was quenched with saturated NH_4Cl (10 mL), and the solvent was evaporated. The product was extracted using ethyl acetate (3×15 mL), and the combined extract was dried over Na_2SO_4, concentrated, dissolved in methanol (8 mL), and the solution was treated with concentrated HCl (1.5 mL). After stirring 2 h at 50 ^oC, the reaction was neutralized using $NaHCO_3$ and methanol was evaporated. Saturated NH_4Cl (10 mL) solution was added, and the product was extracted using ethyl acetate (3×15 mL). The organic layers were combined, washed with brine, dried over Na_2SO_4, concentrated and purified using silica gel column chromatography, eluting with 5:1 dichloromethane-methanol, to provide **35** as white glass (55 mg, 25%). ^1H NMR (300 MHz, methanol-d_4, D_2O) δ 7.36 (s, 1 H), 7.09-7.01 (m, 2 H), 6.97-6.88 (m, 2 H), 6.84 (dq, J = 9.4, 2.6 Hz, 3 H), 6.81-6.73 (m, 2 H), 6.51-6.55 (m, 2 H), 6.50-6.44 (m, 2 H), 6.41 (dt, J = 7.7, 1.3 Hz, 1 H), 4.89 (s, 2 H); ^{13}C NMR (75 MHz, methanol-d_4) δ 158.13, 157.30, 148.54, 145.57, 142.46, 134.75, 134.59, 133.51, 132.90, 131.65, 130.01, 121.14, 117.94, 116.32, 115.26, 52.44; ESIMS *m/z* (relative intensity) 384 (MH^+, 28), 316 (100); negative ion HRESIMS *m/z* calcd for $C_{24}H_{21}N_3O_2$ [$(M - H^+)^-$] 382.1555, found 382.1563. HPLC purity: 100% (C-18 reverse phase, methanol-H_2O, 90:10).

Molecular Docking of Compounds 12 and 36 in the Active Site of Aromatase. The structures of compounds **12** and **36** were constructed with Sybyl 7.1 software and energy minimized to 0.01 kcal/mol by the Powell method using Gasteiger-Huckel charges and the Tripos force field. The crystal structure of aromatase was obtained from the Protein Data Bank (PDB ID: 3s79),[33] and the natural ligand (androstenedione) and all crystal water molecules were removed. Compounds **12** and **36** were docked into the androstenedione binding pocket in aromatase using the GOLD 3.0 program. A distance constraint was added between the imidazole

nitrogen of **12** or **36** and the iron to confine the distance within 1.5-3.5 Å during docking. The best docking solutions according to the GOLD fitness scores were selected.

Molecular Docking of Compound 12 in the Active Site of ER-α. The structure of compound **12** was constructed with Sybyl 7.1 software and energy minimized to 0.01 kcal/mol by the Powell method using Gasteiger-Huckel charges and the Tripos force field. The crystal structure of ER-α was obtained from the Protein Data Bank (PDB ID: 3ert),[34] and the natural ligand (4-hydroxy tamoxifen) and all crystal water molecules (except the water that forms bifurcated hydrogen bonds with Glu353 and Arg394) were removed. Compound **12** was docked into the ligand binding pocket of ER-α using the GOLD 3.0 program. The best docking solution according to GOLD fitness score was selected.

Inhibition of Recombinant Human Aromatase (CYP19) by Microsomal Incubations. The activity of recombinant aromatase (CYP19) was determined by measuring the conversion rate of the fluorometric substrate 7-methoxy-4-trifluoromethylcoumarin (MFC) to its fluorescent metabolite 7-hydroxytrifluoromethylcoumarin (HFC). Experimental procedures were consistent with the published methodology.[37] All of the incubations were performed using incubation times and protein concentrations that were within the linear range for reaction velocity. The fluorometric substrate, MFC, was dissolved in acetonitrile with the final concentration of 25 mM. All tested samples were dissolved in either methanol or DMSO. The sample solutions (2 μL) were mixed well with 98 μL of NADPH-Cofactor Mix (16.25 μM $NADP^+$, 825.14 μM $MgCl_2$, 825.14 μM glucose-6-phosphate and 0.4 Units/mL glucose-6-phosphate dehydrogenase), and were pre-warmed for 10 min at 37 ^oC. Enzyme/substrate mix was prepared with fluorometric substrate, recombinant human aromatase (CYP19) and 0.1 M potassium phosphate buffer (pH 7.4). Reactions were initiated by adding enzyme/substrate mix (100 μL) to bring the incubation

volume to 200 μL, and the mixture was incubated for 30 min. All the reactions were stopped by adding 0.1 M tris base dissolved in acetonitrile (75 μL). The amount of fluorescent product was determined immediately by measuring fluorescent response using a BioTek (Winooski, VT) Synergy 2 fluorometric plate reader. Excitation-emission wavelengths for MFC metabolite were 409 and 530 nm. The standard curve for MFC metabolite was constructed using the appropriate fluorescent metabolite standards. Quantification of samples was performed by applying the linear regression equation of the standard curve to the fluorescence response. The limit of quantification for the metabolites of MFC was 24.7 pmol with intra- and inter-assay coefficients of variation less than 10%. The rates of metabolite formation in the presence of the test inhibitors were compared with those in the control, in which the inhibitor was replaced with vehicle. The extent of enzyme inhibition was expressed as the percentage of remaining enzyme activity compared to the control. IC_{50} values were determined as the inhibitor concentrations that brought about half reduction in enzyme activity by fitting all the data to a one-site competition equation using Graphpad Prism 5.0 (GraphPad Software Inc., San Diego, CA).

Binding Affinities for Recombinant Human ER-α and ER-β. The binding affinities of ER-α and ER-β were determined by measuring the change of polarization value when the fluorescent estrogen ligand, ES2, was displaced by the tested compounds. Experimental procedures were consistent with the protocol provided by Invitrogen. The fluorescent estrogen ligand, ES2, was provided in methanol/water (4:1, v/v) at a concentration of 1800 nM. Recombinant human ER-α and ER-β were provided in buffer (50 mM bis-tris propane, 400 mM KCl, 2 mM DTT, 1 mM EDTA and 10% glycerol), at concentrations of 734 nM and 3800 nM, respectively. All tested samples were dissolved in either methanol or DMSO. The sample solutions (1 μL) were mixed well with 49 μL of ES2 screening buffer (100 mM potassium

phosphate, 100 μg/mL BGG and 0.02% NaN_3). The ER-α/ES2 complex was prepared with the fluorescent estrogen ligand ES2, human recombinant ER and ES2 screening buffer at concentrations of 9 nM ES2 and 30 nM ER-α. The ER-β/ES2 complex was prepared with the fluorescent estrogen ligand ES2, human recombinant ER-β and ES2 screening buffer at concentrations of 9 nM ES2 and 20 nM ER-β. Reactions were initiated by adding ER/ES2 complex (50 μL) to bring the incubation volume to 100 μL, and incubated for 2 h avoiding light. The polarization value was determined by measuring fluorescent response using a BioTek (Winooski, VT) Synergy 2 fluorometric plate reader. Excitation-emission wavelengths for fluorescence polarization were 485 and 530 nM. The polarization values in the presence of the test competitors were compared with those of the control, in which the competitor was replaced with vehicle. The extent of competition was expressed as the percentage of remaining polarization compared to the control. EC_{50} values were determined as the competitor concentrations that brought about half reduction in polarization value by fitting all the data to a one-site competition equation using Graphpad Prism 5.0 (GraphPad Software Inc., San Diego, CA).

Cell Culture and Test Compound Treatment. Estrogen receptor-positive human breast carcinoma cell line (MCF-7 cells) were seeded at a density of 10^5 cells/well in 6-well plates and maintained at 37 ^oC under a humidified atmosphere of 5% CO_2 and 95% air in minimum essential media (MEM) supplemented with 10% fetal bovine serum (FBS). Before the test compound treatments, the cells were preconditioned in charcoal-stripped FBS for 72 h to remove the estrogens from the growth medium containing 10% FBS. The cells were treated with vehicle (0.1% methanol) alone, 1 μM test compound or 1 μM endoxifen (positive control) for 24 h in

the presence of 10 nM β-estradiol (E2) dissolved in MEM supplemented with 10% charcoal-stripped FBS.

Ribonucleic Acid (RNA) Extraction and Concentration Measurement. The MCF-7 cells treated with test compounds or experimental controls for 24 h were harvested for progesterone receptor (PGR) messenger ribonucleic acid (mRNA) extraction. Before ribonucleic acid (RNA) extraction, genomic DNA was eliminated. RNA was extracted from approximately 3×10^5 cells by RNeasy Plus Mini Kit (QiagenInc., Valencia, California, USA). The RNA concentration was measured using the Qubit RNA BR assay (Life Technologies Corp., Carlsbad, CA) for the Qubit 2.0 fluorometer (Life Technologies Corp., Carlsbad, CA). The RNA was stored at –80 ^{o}C before further use.

Complementary Deoxyribonucleic Acid (cDNA) Synthesis. Complementary deoxyribonucleic acid (cDNA) for the real-time quantitative polymerase chain reaction (PCR) assay was synthesized from DNase-treated total RNA using the QuantiTect reverse transcription kit (QiagenInc., Valencia, California, USA).

Real-Time Quantitative Polymerase Chain Reaction (PCR) for cDNA. The cDNA was amplified with TaqMan Universal PCR Master Mix (Applied Biosystems Inc., Carlsbad, CA), and then PCR was performed in the QuantStudio 12K Flex Real-Time PCR System (Life Technologies Corp., Carlsbad, CA). Progesterone receptor gene (PGR, FAM, Hs01556702, Life Technologies Corp., Carlsbad, CA) was the target gene, while glyceraldehyde-3-phosphate dehydrogenase (GAPDH, VIC, Hs02758991, Life Technologies Corp., Carlsbad, CA) gene expression was quantified to normalize each sample. A total of 40 amplification cycles were performed. Quantitative values of amplification were obtained from the threshold cycle (*Ct*) defined as the cycle number at which the fluorescent signal is first recorded above the

background as determined during the exponential phase of PCR rather than at the endpoint. The $2^{-\Delta\Delta Ct}$ method was used to determine the relative mRNA expression, and the results were expressed as percentages of antagonism effects compared to E2-stimulated PGR mRNA expression (considered as 100%). If amplification was not seen by 40 cycles, the measured RNA was considered to be undetectable.

AUTHOR INFORMATION

Corresponding Author

* Tel: 765-494-1465. Fax: 765-494-6790. E-mail: cushman@purdue.edu.

Notes

The authors declare no competing financial interest.

ACKNOWLEDGMENT

This research was supported by the Purdue University Center for Cancer Research and the Indiana University Cancer Center Joint Funding Award 206330, by the Purdue Center for Cancer Research grant P30 CA023168, by a Purdue Research Foundation Research Grant, and by an award from the Floss Endowment, provided to the Department of Medicinal Chemistry and Molecular Pharmacology, Purdue University. W. Lv also thanks Dr. Charles Paget for providing a graduate travel award.

ABBREVIATIONS USED

AIs, aromatase inhibitors; SERMs, selective estrogen receptor modulators; ATAC, arimidex, tamoxifen, alone or in combination; ER, estrogen receptor; FDA, Food and Drug Administration;

MOMCl, methyl chloromethyl ether; NBS, *N*-bromosuccinimide; CYP, cytochrome P450; E2, β-estradiol; PGR, progesterone receptor; PDB, protein data bank.

ASSOCIATED CONTENT

Supporting Information

(1) SMILES molecular formula strings (CSV). (2) Molecular models of compound **12** in the active sites of aromatase and ER-α, and associated tables listing hydrogen bond angles. This material is available free of charge via the Internet at http://pubs.acs.org.

REFERENCES

1. Ghosh, D.; Griswold, J.; Erman, M.; Pangborn, W. Structural Basis for Androgen Specificity and Oestrogen Synthesis in Human Aromatase. *Nature* **2009**, *457*, 219-223.
2. Bonneterre, J.; Buzdar, A.; Nabholtz, J. M. A.; Robertson, J. F. R.; Thurlimann, B.; von Euler, M.; Sahmoud, T.; Webster, A.; Steinberg, M.; Arimidex Writing, C.; Investigators Comm, M. Anastrozole is Superior to Tamoxifen as First-line Therapy in Hormone Receptor Positive Advanced Breast Carcinoma - Results of Two Randomized Trials Designed for Combined Analysis. *Cancer* **2001**, *92*, 2247-2258.
3. Mouridsen, H.; Gershanovick, M.; Sun, Y.; Perez-Carrion, R.; Boni, C.; Monnier, A.; Apffelstaedt, J.; Smith, R.; Sleeboom, H. P.; Jaenicke, F.; Pluzanska, A.; Dank, M.; Becquart, D.; Bapsy, P. P.; Salminen, E.; Snyder, R.; Chaudri-Ross, H.; Lang, R.; Wyld, P.; Bhatnagar, A. Phase III Study of Letrozole Versus Tamoxifen as First-line Therapy of Advanced Breast Cancer in Postmenopausal Women: Analysis of Survival and Update of Efficacy from the International Letrozole Breast Cancer Group. *J. Clin. Oncol.* **2003**, *21*, 2101-2109.
4. Howell, A.; Cuzick, J.; Baum, M.; Buzdar, A.; Dowsett, M.; Forbes, J. F.; Hoctin-Boes, G.; Houghton, I.; Locker, G. Y.; Tobias, J. S.; Grp, A. T. Results of the ATAC (Arimidex, Tamoxifen, Alone or in Combination) Trial after Completion of 5 Years' Adjuvant Treatment for Breast Cancer. *Lancet* **2005**, *365*, 60-62.
5. Thurlimann, B.; Keshaviah, A.; Coates, A. S.; Mouridsen, H.; Mauriac, L.; Forbes, J. F.; Paridaens, R.; Castiglione-Gertsch, M.; Gelber, R. D.; Rabaglio, M.; Smith, I.; Wardly, A.; Price, K. N.; Goldhirsch, A.; Grp, B. I. G. C. A Comparison of Letrozole and

Tamoxifen in Postmenopausal Women with Early Breast Cancer. *N. Engl. J. Med.* **2005**, *353*, 2747-2757.

6. Williams, N. Effect of Anastrozole and Tamoxifen as Adjuvant Treatment for Early-stage Breast Cancer: 100-Month Analysis of the ATAC Trial. *Lancet Oncol.* **2008**, *9*, 45-53.
7. Heshmati, H. M.; Khosla, S.; Robins, S. P.; O'Fallon, W. M.; Melton, L. J.; Riggs, B. L. Role of Low Levels of Endogenous Estrogen in Regulation of Bone Resorption in Late Postmenopausal Women. *J. Bone Miner. Res.* **2002**, *17*, 172-178.
8. Ewer, M. S.; Gluck, S. A Woman's Heart. The Impact of Adjuvant Endocrine Therapy on Cardiovascular Health. *Cancer* **2009**, *115*, 1813-1826.
9. Bird, B. R. J. H.; Swain, S. M. Cardiac Toxicity in Breast Cancer Survivors: Review of Potential Cardiac Problems. *Clin. Cancer Res.* **2008**, *14*, 14-24.
10. Bundred, N. J. The Effects of Aromatase Inhibitors on Lipids and Thrombosis. *Br. J. Cancer* **2005**, *93*, S23-S27.
11. Khan, Q. J.; O'Dea, A. P.; Sharma, P. Musculoskeletal Adverse Events Asociated with Adjuvant Aromatase Inhibitors. *J. Oncol.* **2010**, 8 pages.
12. Henry, N. L.; Giles, J. T.; Ang, D.; Mohan, M.; Dadabhoy, D.; Robarge, J.; Hayden, J.; Lemler, S.; Shahverdi, K.; Powers, P.; Li, L.; Flockhart, D.; Stearns, V.; Hayes, D. F.; Storniolo, A. M.; Clauw, D. J. Prospective Characterization of Musculoskeletal Symptoms in Early Stage Breast Cancer Patients Treated with Aromatase Inhibitors. *Breast Cancer Res. Treat.* **2008**, *111*, 365-372.
13. Henry, N. L.; Jacobson, J. A.; Banerjee, M.; Hayden, J.; Smerage, J. B.; Van Poznak, C.; Storniolo, A. M.; Stearns, V.; Hayes, D. F. A Prospective Study of Aromatase Inhibitor-

Associated Musculoskeletal Symptoms and Abnormalities on Serial High-Resolution Wrist Ultrasonography. *Cancer* **2010**, *116*, 4360-4367.

14. Gaillard, S.; Stearns, V. Aromatase Inhibitor-associated Bone and Musculoskeletal Effects: New Evidence Defining Etiology and Strategies for Management. *Breast Cancer Res.* **2011**, *13:205*.

15. Sedjo, R. L.; Devine, S. Predictors of Non-adherence to Aromatase Inhibitors Among Commercially Insured Women with Breast Cancer. *Breast Cancer Res. Treat.* **2011**, *125*, 191-200.

16. Partridge, A. H.; LaFountain, A.; Mayer, E.; Taylor, B. S.; Winer, E.; Asnis-Alibozek, A. Adherence to Initial Adjuvant Anastrozole Therapy Among Women with Early-stage Breast Cancer. *J. Clin. Oncol.* **2008**, *26*, 556-562.

17. Jelovac, D.; Macedo, L.; Goloubeva, O. G.; Handratta, V.; Brodie, A. M. H. Additive Antitumor Effect of Aromatase Inhibitor Letrozole and Antiestrogen Fulvestrant in a Postmenopausal Breast Cancer Model. *Cancer Res.* **2005**, *65*, 5439-5444.

18. Mehta, R. S.; Barlow, W. E.; Albain, K. S.; Vandenberg, T. A.; Dakhil, S. R.; Tirumali, N. R.; Lew, D. L.; Hayes, D. F.; Gralow, J. R.; Livingston, R. B.; Hortobagyi, G. N. Combination Anastrozole and Fulvestrant in Metastatic Breast Cancer. *New Engl. J. Med.* **2012**, *367*, 435-444.

19. Macedo, L. F.; Sabnis, G. J.; Goloubeva, O. G.; Brodie, A. M. H. Combination of Anastrozole with Fulvestrant in the Intratumoral Aromatase Xenograft Model. *Cancer Res.* **2008**, *68*, 3516-3522.

20. Baum, M.; Buzdar, A. U.; Cuzick, J.; Forbes, J.; Houghton, J.; Klijn, J. G. M.; Sahmoud, T.; Grp, A. T. Anastrozole Alone or in Combination with Tamoxifen Versus Tamoxifen

Alone for Adjuvant Treatment of Postmenopausal Women with Early Breast Cancer: First Results of the ATAC Randomised Trial. *Lancet* **2002**, *359*, 2131-2139.

21. Gruber, C. J.; Tschugguel, W.; Schneeberger, C.; Huber, J. C. Mechanisms of Disease - Production and Actions of Estrogens. *New Engl. J. Med.* **2002**, *346*, 340-352.

22. Baum, M.; Dowsett, M.; Coibion, M.; Bianco, A. R.; Cuzick, J.; George, W. D.; Gray, J.; Howell, A.; Houghton, J.; Williams, N.; Sloane, J.; Tobias, J.; Buzdar, A.; Anderson, M. D.; Jackson, I.; Sahmoud, T.; Gallagher, J.; Webster, A.; Gangji, D.; Petrakova, K.; Konopasek, B.; Mares, P.; Vodvarka, P.; Alcazar, A.; Campos, O.; Maxwell, A.; Goedhals; Hacking, D.; Landers, G.; Smith, L.; Vorobiof, D. A.; Werner, I. D.; Blamey, R.; Coleman, R.; Grieve, R. J.; Hickish, T.; Howell, A.; Nicholls, J. C.; Nicholson, S.; Raymond, S.; Salman, A.; Blum, J.; Clark, R.; Lyss, A.; Miletello, G.; Sternberg, J.; Forbes, J.; Coibion, M.; Nabholtz, J. M.; Guastalla, J. P.; Distler, W.; Klijn, J. G. M.; Nagykalnai, T.; Nicolucci, A.; Bianco, A. R.; Constenla, M.; Nylen, U.; Howell, A.; Sainsbury, R.; Mansel, R. E.; Goerge, D.; Buzdar, A. U.; Locker, G. Y.; Gallagher, J.; Jackson, I.; Sahmoud, T.; Houghton, J.; Williams, N.; Nicolucci, A.; Pollard, S.; Stroner, P.; Buyse, M.; Margolese, R.; Northover, J. M. A. Pharmacokinetics of Anastrozole and Tamoxifen Alone, and in Combination, During Adjuvant Endocrine Therapy for Early Breast Cancer in Postmenopausal Women: a Sub-protocol of the 'Arimidex (TM) and Tamoxifen Alone or in Combination' (ATAC) Trial. *Br. J. Cancer* **2001**, *85*, 317-324.

23. Lu, W. J.; Xu, C.; Pei, Z. F.; Mayhoub, A. S.; Cushman, M.; Flockhart, D. A. The Tamoxifen Metabolite Norendoxifen Is a Potent and Selective Inhibitor of Aromatase (CYP19) and a Potential Lead Compound for Novel Therapeutic Agents. *Breast Cancer Res. Treat.* **2012**, *133*, 99-109.

24. Lv, W.; Liu, J.; Lu, D.; Flockhart, D. A.; Cushman, M. Synthesis of Mixed (*E*,*Z*)-, (*E*)-, and (*Z*)-Norendoxifen with Dual Aromatase Inhibitory and Estrogen Receptor Modulatory Activities. *J. Med. Chem.* **2013**, *56*, 4611-4618.

25. Liu, J. Z.; Flockhart, P. J.; Lu, D. S.; Lv, W.; Lu, W. J. J.; Han, X.; Cushman, M.; Flockhart, D. A. Inhibition of Cytochrome P450 Enzymes by the E- and Z-Isomers of Norendoxifen. *Drug Metab. and Dispos.* **2013**, *41*, 1715-1720.

26. Lv, W.; Liu, J. Z.; Skaar, T. C.; Flockhart, D. A.; Cushman, M. Design and Synthesis of Norendoxifen Analogues with Dual Aromatase Inhibitory and Estrogen Receptor Modulatory Activities. *J. Med. Chem.* **2015**, *58*, 2623-2648.

27. Winkler, V. W.; Nyman, M. A.; Egan, R. S. Diethylstilbestrol Cis-trans Isomerization and Estrogen Activity of Diethylstilbestrol Isomers. *Steroids* **1971**, *17*, 197-&.

28. Katzenellenbogen, J. A.; Carlson, K. E.; Katzenellenbogen, B. S. Facile Geometric Isomerization of Phenolic Non-Steroidal Estrogens and Antiestrogens: Limitations to the Interpretation of Experiments Characterizing the Activity of Individual Isomers. *J. Steroid Biochem. Mol. Biol.* **1985**, *22*, 589-596.

29. Robertson, D. W.; Katzenellenbogen, J. A.; Long, D. J.; Rorke, E. A.; Katzenellenbogen, B. S. Tamoxifen Antiestrogens. A Comparison of the Activity, Pharmacokinetics, and Metabolic Activation of the Cis and Trans Isomers of Tamoxifen. *J. Steroid Biochem. Mol. Biol.* **1982**, *16*, 1-13.

30. Williams, M. L.; Lennard, M. S.; Martin, I. J.; Tucker, G. T. Interdividual Variation in the Isomerization of 4-Hydroxytamoxifen by Human Liver Microsomes: Involvement of Cytochromes P450. *Carcinogenesis* **1994**, *15*, 2733-2738.

31. Lubczyk, V.; Bachmann, H.; Gust, R. Investigations on Estrogen Receptor Binding. The Estrogenic, Antiestrogenic, and Cytotoxic Properties of C2-Alkyl-Substituted 1,1-Bis(4-hydroxyphenyl)-2-phenylethenes. *J. Med. Chem.* **2002**, *45*, 5358-5364.

32. Lim, Y. C.; Desta, Z.; Flockhart, D. A.; Skaar, T. C. Endoxifen (4-Hydroxy-*N*-desmethyl-tamoxifen) Has Anti-estrogenic Effects in Breast Cancer Cells with Potency Similar to 4-Hydroxy-tamoxifen. *Cancer Chemother. Pharmacol.* **2005**, *55*, 471-478.

33. Ghosh, D.; Lo, J.; Morton, D.; Valette, D.; Xi, J.; Griswold, J.; Hubbell, S.; Egbuta, C.; Jiang, W.; An, J.; Davies, H. M. L. Novel Aromatase Inhibitors by Structure-Guided Design. *J. Med. Chem.* **2012**, *55*, 8464-8476.

34. Shiau, A. K.; Barstad, D.; Loria, P. M.; Cheng, L.; Kushner, P. J.; Agard, D. A.; Greene, G. L. The Structural Basis of Estrogen Receptor/Coactivator Recognition and the Antagonism of This Interaction by Tamoxifen. *Cell* **1998**, *95*, 927-937.

35. Miyano, M.; Deason, J. R. Preparationo of Phenolic Ester Derivatives as Elastase Inhibitors. US4633241A, July 28, 1987, 1987.

36. Simmons, E. M.; Hartwig, J. F. Iridium-Catalyzed Arene Ortho-Silylation by Formal Hydroxyl-Directed C-H Activation. *J. Amer. Chem. Soc.* **2010**, *132*, 17092-17095.

37. Lu, W. J.; Ferlito, V.; Xu, C.; Flockhart, D. A.; Caccamese, S. Enantiomers of Naringenin as Pleiotropic, Stereoselective Inhibitors of Cytochrome P450 Isoforms. *Chirality* **2011**, *23*, 891-896.

TOC Graphic

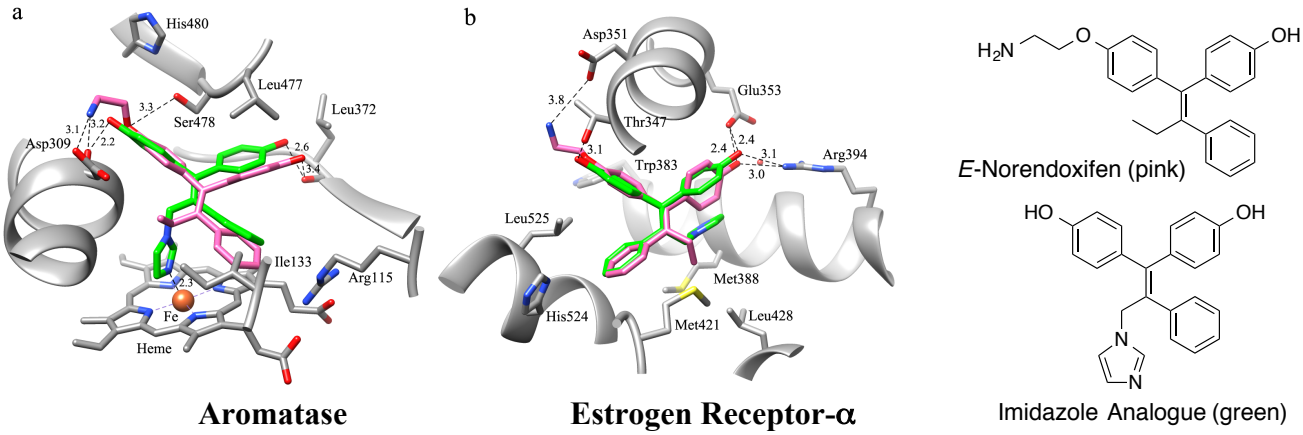

Aromatase **Estrogen Receptor-α**